

1 **Powdery mildew infection induces a non-canonical route to storage lipid formation at the**  
2 **expense of host thylakoid lipids to fuel its spore production**

3  
4 **J. Jaenisch<sup>1a</sup>, H. Xue<sup>1a</sup>, J. Schläpfer<sup>2b</sup>, E.R. McGarrigle<sup>1</sup>, K. Louie<sup>3</sup>, T.R. Northen<sup>2-3</sup>, M.C.**  
5 **Wildermuth<sup>1\*</sup>**

6 <sup>1</sup>Department of Plant and Microbial Biology, University of California, Berkeley, CA 94720

7 <sup>2</sup>Environmental Genomics and Systems Biology Division, Lawrence Berkeley National Laboratory, 1 Cyclotron  
8 Road, Berkeley, CA 94720

9 <sup>3</sup>The DOE Joint Genome Institute, Lawrence Berkeley National Laboratory, 1 Cyclotron Road, Berkeley, CA 94720

10 <sup>a</sup>Authors contributed equally to this work

11 <sup>b</sup>Present address: Department of Plant and Microbial Biology, University of Zurich, Zurich 8008

12 **\* Corresponding author's email address:** Mary. C. Wildermuth, [mwildermuth@berkeley.edu](mailto:mwildermuth@berkeley.edu)

13

14 **Running title:** Plastid TAGs fuel powdery mildew spore production

15 The author(s) responsible for distribution of materials integral to the findings presented in this article in accordance  
16 with the policy described in the Instructions for Authors (<https://academic.oup.com/plcell/pages/General-Instructions>) is (are): Mary. C. Wildermuth ([mwildermuth@berkeley.edu](mailto:mwildermuth@berkeley.edu))

18

19 **ABSTRACT**

20 Powdery mildews are obligate biotrophic fungi that manipulate plant metabolism to supply  
21 lipids, particularly during fungal asexual reproduction when fungal lipid demand is extensive.  
22 The mechanism for host response to fungal lipid demand has not been resolved. We found  
23 storage lipids, triacylglycerols (TAGs), increase by 3.5-fold in powdery mildew-infected tissue.  
24 In addition, lipid bodies, not observable in uninfected mature leaves, are present in both cytosol  
25 and chloroplasts at the infection site. This is concurrent with decreased thylakoid membrane  
26 lipids and thylakoid disassembly. Together, these findings indicate that the powdery mildew  
27 induces localized thylakoid membrane degradation to promote storage lipid formation. Genetic  
28 analyses show the canonical ER pathway for TAG synthesis does not support powdery mildew  
29 spore production. Instead, *Arabidopsis DIACYLGLYCEROL ACYLTRANSFERASE 3*  
30 (DGAT3), shown to be chloroplast-localized and to be largely responsible for powdery mildew-  
31 induced chloroplast TAGs, promotes fungal asexual reproduction. Powdery mildew-induced leaf  
32 TAGs are enriched in thylakoid associated fatty acids, which are also present in the produced  
33 spores. This research provides new insights on obligate biotrophy and plant lipid metabolism  
34 plasticity and function. Furthermore, by understanding how photosynthetically active leaves can  
35 be converted into TAG producers, more sustainable and environmentally benign plant oil  
36 production could be facilitated.

37

38

39

40 **INTRODUCTION**

41

42 As obligate biotrophic pathogens, powdery mildews acquire nutrients supplied by living  
43 host cells to support their life cycle and have specialized strategies for maximizing the output of  
44 these tissues (Glawe 2008; Wildermuth et al. 2017). In the *Arabidopsis thaliana*-*Golovinomyces*  
45 *orontii* interaction, the establishment of the fungal feeding structure, called a haustorium, occurs  
46 by 24 hours post inoculation (hpi). By 5 days post inoculation (dpi), asexual reproductive  
47 structures called conidiophores form. These conidiophores contain chains of conidia which store  
48 energy in the form of lipids and glycogen (Both et al. 2005; Micali et al. 2008). Thus, the fungal  
49 demand for nutrients is especially high during asexual reproduction. As a response to the  
50 nutritional demands, a metabolic switch occurs in the host infected leaves. Mature leaves are  
51 considered source tissues producing hexoses for transport to growing parts of the plant.  
52 However, powdery mildew infection induces localized signatures of mobilization of  
53 carbohydrates to the tissue underlying the fungal infection site, for fungal acquisition (Clark and  
54 Hall 1998; Sutton, Henry, and Hall 1999; Fotopoulos et al. 2003; Swarbrick, Schulze-Lefert, and  
55 Scholes 2006). Furthermore, localized transcriptome profiling using laser microdissection shows  
56 the expression of genes associated with enhanced glycolysis and respiration to be increased,  
57 while the expression of chlorophyll biosynthesis genes is decreased at the powdery mildew  
58 infection site, in support of a localized source to sink transition (Chandran et al. 2010). Analysis  
59 of powdery mildew genomes found reduced carbohydrate metabolism pathways but relatively  
60 complete fatty acid (FA) metabolism and utilization pathways, suggesting lipids may be a  
61 preferred nutrient (Liang et al. 2018). And, an early study found enhanced lipid accumulation in  
62 powdery mildew infected cucumber leaves compared to uninfected leaves (Abood and Lösel  
63 1989).

64 Microbial acquisition of host lipids has emerged as a common strategy across host-  
65 microbe systems, particularly for obligate biotrophs including human intracellular pathogens  
66 (Atella et al. 2009; Costa et al. 2018). For plant obligate biotrophs, the arbuscular mycorrhizal  
67 fungi (AMF) symbiosis in which AMF colonize plant roots, providing minerals to the plant host  
68 while acquiring host sugars and lipids is best studied (MacLean, Bravo, and Harrison 2017;  
69 Luginbuehl et al. 2017; Kameoka and Gutjahr 2022). AMF induce a specific shift in host lipid  
70 metabolism, catalyzed by enzymes specific to plants colonized by AMF, to yield 2-  
71 monoacylglycerols (2-MG), with C16:0 2-MGs preferred. While 2-MGs appear to be the likely

72 final product transferred to AMF, this has not been verified, and it is possible other lipids may  
73 also be transported particularly if acquisition is facilitated by exocytotic vesicles. Once these host  
74 lipids are acquired, they are remodeled by the AMF and stored primarily as TAGs in lipid bodies  
75 for future use.

76 By contrast with the AMF symbiosis, almost nothing is known about how the powdery  
77 mildew fungus manipulates host metabolism for fungal lipid acquisition. Because powdery  
78 mildews have the capacity to synthesize FAs, unlike AMF which are FA auxotrophs (Kameoka  
79 and Gutjahr 2022), we focus our studies on powdery mildew-infected leaves during powdery  
80 mildew asexual reproduction (5+ dpi), when spores replete with lipid bodies (Both et al., 2005)  
81 are formed. We reason that host lipids would be most in demand at this phase of the powdery  
82 mildew life cycle. Furthermore, Jiang and colleagues, as part of their research on AMF, show  
83 host FA manipulation is reflected in powdery mildew spore FAs (Jiang et al. 2017). Specifically,  
84 their introduction of UcFatB, a fatty acid thioesterase that terminates FA elongation early,  
85 terminating with C12:0, into *Arabidopsis* resulted in increased C12:0 FAs in both host leaves and  
86 powdery mildew spores.

87 Plant lipid metabolism is dynamic across developmental stages and responsive to  
88 environmental stimuli, modifying energy content of storage tissues, altering membrane fluidity at  
89 different temperatures, minimizing lipotoxicity, and providing chemical signals (Baud et al.  
90 2008; Moellering, Muthan, and Benning 2010; Okazaki and Saito 2014; Cavaco, Matos, and  
91 Figueiredo 2021). In plants such as *Arabidopsis*, acyl-chains are produced in chloroplasts, with  
92 the exception of a small fraction generated in mitochondria, and their subsequent assembly into  
93 lipids occurs via pathways operating in the chloroplast (prokaryotic pathway) and the  
94 endoplasmic reticulum (eukaryotic pathway). In *Arabidopsis* leaves, approximately 38% of  
95 newly synthesized FAs are utilized in the prokaryotic lipid-synthesis pathway, whereas the  
96 remaining 62% are directed towards the eukaryotic pathway (Browse et al. 1986). A portion of  
97 acyl-chains from ER-assembled lipids are subsequently transported – likely as PA and/or DAG –  
98 back to the plastid to serve as substrates for thylakoid lipid synthesis (Yao et al. 2023; Hölzl and  
99 Dörmann 2019). Triacylglycerols (TAGs), neutral storage lipids with three fatty acids attached to  
100 a glycerol backbone, are packaged into lipid bodies. Eukaryotes synthesize TAGs in the ER via  
101 two major pathways: the Kennedy pathway and the acyl-CoA independent pathway (C. Xu, Fan,  
102 and Shanklin 2020). Diacylglycerol acyltransferases (DGAT, EC 2.3.1.20) catalyze the final and

103 rate-limiting step in TAG synthesis forming TAG from diacylglycerol (DAG) and acyl-CoA in  
104 the Kennedy pathway. Whereas, phospholipid:diacylglycerol acyltransferase (PDAT, EC  
105 2.3.1.158) catalyzes the final and rate-limiting step in acyl-CoA independent TAG synthesis with  
106 TAG formed from DAG and a phospholipid (PL) acyl donor, i.e. phosphatidylcholine (PC)  
107 remodeled from the Lands Cycle (Dahlqvist et al. 2000; Zhang et al. 2009; L. Wang et al. 2012).

108 In this study, we show powdery mildew-induced TAG accumulation in mature  
109 *Arabidopsis thaliana* leaves occurs at the infection site concurrent with powdery mildew asexual  
110 reproduction. We employ genetic, microscopic, and lipidomic approaches to uncover a non-  
111 canonical route for plant TAG synthesis via AtDGAT3 to support powdery mildew spore  
112 formation. AtDGAT3 is unusual in that, unlike the ER membrane proteins DGAT1 and DGAT2,  
113 it is a soluble metalloprotein containing a [2Fe-2S] cluster (Aymé et al. 2014). We show  
114 AtDGAT3 is localized to the chloroplast and responsible for plastidic TAG synthesis that occurs  
115 at the expense of thylakoid membranes. We further speculate on controls over functional roles of  
116 ER- versus chloroplast- derived lipid bodies in the powdery mildew interaction, powdery mildew  
117 acquisition of the chloroplast-derived lipid bodies, and controls over AtDGAT3 stability and  
118 activity. Our findings open further avenues of investigation with respect to biotroph-host  
119 interactions and plant response to stress or aging (e.g. leaf senescence). Moreover, this work  
120 could facilitate more sustainable production of vegetable oil, biofuels and other specialty  
121 chemicals (X.-Y. Xu et al. 2018).

122

## 123 **RESULTS**

### 124 **Powdery mildew infection increases triacylglycerols in the host leaf while phospholipids 125 decrease**

126 Powdery mildew fungi are obligate biotrophs that rely entirely on the host for nutrients.  
127 Powdery mildew asexual reproduction creates a high metabolic demand for lipids as the powdery  
128 mildew feeding structures, haustoria, and newly formed spores are filled with lipid bodies at 5  
129 dpi when asexual reproduction is first apparent (**Fig. 1, A-C**).

130 To understand how host lipid metabolism is manipulated to meet this fungal lipid  
131 demand, we performed lipid profiling of uninfected and parallel powdery mildew-infected leaves  
132 at 12 days post inoculation (dpi). This later time point exhibits sufficient powdery mildew

133 proliferation to allow us to assess the impact of the powdery mildew in whole leaf analyses.  
134 Lipids were extracted and identified by LC-MS/MS fragmentation patterns (**Supplemental Fig.**  
135 **1, Supplemental Dataset 1**). Our results show that TAGs increase in 12 dpi washed leaf extracts  
136 relative to uninfected leaf extracts, with a 3.5-fold increase in abundance (**Fig. 1D**). Overall,  
137 there is a shift to TAGs containing longer acyl chains, including very long chain fatty acids  
138 (VLCFA,  $\geq$ C20), assessed at  $\geq$ C56:x, which increase 7-fold with infection (**Fig. 1E-F**,  
139 **Supplemental Fig. S1; Supplemental Dataset 1**). Examination of the most abundant TAG  
140 class, C54:x, shows an increase of 3.5-fold with infection accompanied by a shift towards a more  
141 desaturated profile in infected leaves (**Fig. 1F-G**); this reflects increased 18:3 and 18:2 FA  
142 composition (**Supplemental Dataset 1**).

143 While TAGs increase, phospholipids decrease in abundance in extracts from infected  
144 leaves at 12 dpi compared to parallel uninfected leaves (**Fig. 1H, Supplemental Dataset 1**).  
145 Phosphatidylcholine (PC), the dominant phospholipid in mature *Arabidopsis* leaves, decreases by  
146 30%. Phosphatidylethanolamine (PE) and phosphatidylglycerol (PG) decrease by 50% and 60%  
147 respectively in infected leaves. Although a net decrease in total phosphatidylinositol (PI) with  
148 infection of 20% is observed, it is not statistically significant. Lysophosphatidylcholines (LPC)  
149 increase by ~4-fold in infected leaves. The observed decrease in PC is consistent with increased  
150 TAG synthesis utilizing DAG formed from PC (and PA) via DGATs. The decreases in the other  
151 phospholipids (PE, PI, PG) may facilitate increased flux to TAG accumulation. Furthermore, the  
152 indication that LPC increases at 12 dpi suggests possible operation of the Lands Cycle using  
153 PDAT1.

154 In summary, our data indicates that the powdery mildew remodels host lipid metabolism  
155 to promote localized TAG accumulation.

156 **Genetic analyses indicate the canonical route for plant TAG synthesis in the ER hinders**  
157 **powdery mildew asexual reproduction while chloroplast-localized DGAT3 promotes it**

158 We next examined the impact of genes encoding proteins catalyzing the final and rate-  
159 limiting step in canonical TAG biosynthesis in the ER (Vanhercke et al. 2019) on powdery  
160 mildew spore production, *AtDGAT1* (*At2g19450*), *AtDGAT2* (*At3g51520*), and *AtPDAT1*  
161 (*At5g13640*), using *Arabidopsis* null mutants and/or spray-induced gene silencing (SIGS). Our  
162 employed SIGS methodology specifically silences targeted genes with minimal off targets

163 (Methods; McRae et al. 2023). Furthermore, the *Arabidopsis* DGATs evolved independently,  
164 contain distinct functional domains, and share little sequence similarity (Yin et al. 2022). In seed  
165 oil accumulation, AtDGAT1 and AtPDAT1 play dominant roles. A null mutant in *AtDGAT1*  
166 shows a 30% reduction in seed TAGs, while RNAi silencing of *PDAT1* in a *dgat1-1* background  
167 or *DGAT1* in *pdat1-1* background results in 70 to 80% decreases in seed oil content (Katavic et  
168 al. 1995; Zhang et al. 2009). While it doesn't contribute to seed TAG accumulation, AtDGAT2,  
169 along with AtDGAT1 and AtPDAT1, can impact leaf TAG accumulation (Zhou et al. 2013; Fan,  
170 Yan, and Xu 2013). Furthermore, we explored the impact of ATP-binding cassette A 9  
171 (ABCA9), demonstrated to import FA/acyl-CoA into the ER and to exhibit a 35% reduction in  
172 seed TAG accumulation in the *abca9-1* mutant (Kim et al. 2013). The ER-localized long-chain  
173 acyl-CoA synthetase 1 (LACS1) was also investigated because it acts on long chain and very  
174 long chain FAs (Lü et al. 2009) which we observed to increase with infection (**Fig. 1E-F**) and is  
175 the only ER-localized LACS (Zhao et al. 2010) with enhanced expression at the powdery mildew  
176 infection site at 5 dpi (Chandran et al. 2010).

177 To our surprise, *dgat1-1* and *abca9-1* null mutants allow for enhanced powdery mildew  
178 spore production, 24% and 50% more, respectively, than wild type (WT) plants, whereas, the  
179 *lacs1-1* and *pdat1-2* mutants show no significant change in spore production (**Fig. 2A**).  
180 Knockdown of *AtDGAT1* via SIGS results in more than 60% increase in spore production,  
181 whereas, silencing of *AtDGAT2* shows no difference in spore production from mock treatment  
182 (**Fig. 2B**). Taken together, our findings indicate that TAG synthesis in the ER, using the FA  
183 importer ABCA9 and DGAT1, is not used to support powdery mildew spore production, but  
184 instead hinders it.

185 While AtDGAT1 and AtDGAT2 are ER-localized and membrane-bound, the third  
186 *Arabidopsis* DGAT protein, AtDGAT3, contains a predicted N-terminal chloroplast transit  
187 peptide (cTP) and no transmembrane domain (Aymé et al. 2018). AtDGAT3 was initially shown  
188 to be localized to the cytosol (Hernández et al. 2012), but this study utilized an N-terminus  
189 truncated form of the enzyme lacking the cTP. By contrast with *DGAT1*, targeting *DGAT3* via  
190 SIGS reduces spore production by 40% (**Fig. 2B**). To confirm the impact of *DGAT3* reduction on  
191 powdery mildew asexual reproduction, we obtained a homozygous null mutant in *AtDGAT3*,  
192 *dgat3-2* (**Supplemental Fig S2**). *dgat3-2* plants support 21% less spore production than WT  
193 (**Fig. 2B**). The larger impact on spore production shown with SIGS rather than null mutants in

194 *DGAT1* and *DGAT3* may be due to genetic compensation through development in the null  
195 mutant plants. Neither *dgat1-1* nor *dgat3-2* plants exhibit any obvious developmental or  
196 morphological phenotypes.

197 To determine the localization of AtDGAT3, we cloned the genomic DNA encoding the  
198 full length AtDGAT3 sequence and fused 35S to its N-terminus and GFP to its C-terminus.  
199 Transient expression of *AtDGAT3-GFP* in *Nicotiana benthamiana* leaves via *Agrobacterium*  
200 infiltration results in intense GFP fluorescence that is colocalized with chlorophyll  
201 autofluorescence, indicating *DGAT3* is localized to chloroplasts (**Fig. 2C**).

202 **Figure 2D** places the tested players in the context of integrated chloroplast-ER lipid  
203 metabolism focused on TAG synthesis (Browse et al. 1986; Hörlz and Dörmann 2019; C. Xu,  
204 Fan, and Shanklin 2020; Vanhercke et al. 2019), with the addition of AtDGAT3 chloroplast  
205 localization. In summary, leaf TAG synthesis to support powdery mildew asexual reproduction  
206 occurs using a novel route via DGAT3 in the chloroplast. By contrast, canonical TAG synthesis  
207 in the ER via DGAT1 limits spore production.

## 208 Powdery mildew- induced host lipid bodies are present both in the cytosol and chloroplasts

209 Given our finding that plastidic DGAT3 supports powdery mildew spore production, we  
210 performed confocal imaging of infected leaf tissue at 5 and 10 dpi stained with the neutral lipid  
211 dye BODIPY505/515 and focused on mesophyll cells underlying powdery mildew feeding  
212 structures. As *Arabidopsis* RPW8.2 is specifically targeted to the fungal extrahaustorial  
213 membrane (EHM), we infected Col-0 lines expressing RPW8.2-YFP with *G. orontii* to visualize  
214 the haustorium (W. Wang et al. 2009). The haustorium resides in the epidermal cell as depicted  
215 in **Fig. 1A** and is located above three mesophyll cells (**Fig. 3A**). At the infection site at 5 dpi,  
216 abundant lipid droplets are highly localized to the three mesophyll cells right underneath the  
217 haustorium (white dashed line in **Fig. 3B**) and not in distal cells. Almost no lipid bodies are  
218 observed in parallel uninfected tissue mesophyll cells. As the infection progresses to 10 dpi, the  
219 abundance of lipid bodies increases in the neighboring mesophyll cells. The percent area with  
220 fluorescence shows a ~6-fold increase with infection at 5 dpi and ~15-fold increase with  
221 infection at 10 dpi (**Fig. 3C**). BODIPY505/515-stained lipid bodies are observed both next to  
222 chloroplasts and in the cytoplasm. With closer examination using 3D reconstructions of multiple  
223 z-stacked confocal images, we observe that some infection induced lipid bodies are embedded in

224 the chloroplast (**Fig. 3D**, yellow circled). These chloroplast-embedded lipid bodies (5.2 and 5.9  
225  $\mu\text{m}$  diameter) are similar in size to those that are not embedded; chloroplast adjacent lipid body  
226 mean diameter is 3.7 $\mu\text{m}$  ( $n = 8$ ) and cytoplasmic lipid body mean diameter is 3.4  $\mu\text{m}$  ( $n=5$ ).  
227 Together, our results indicate that powdery mildew infection shifts host lipid metabolism to form  
228 large storage lipid bodies with some of the lipid bodies inside chloroplasts, others adjacent to or  
229 very near the chloroplast, and others in the cytosol.

### 230 **Chloroplast TAG accumulation, but not host defense, is altered in *dgat3-2***

231 To directly assess whether DGAT3 impacts powdery mildew-induced TAG formation,  
232 we performed lipid extractions on 12 dpi leaves and isolated chloroplasts from 12 dpi leaves of  
233 *dgat3-2* and WT plants. Using thin layer chromatography (TLC) we find that the TAG content of  
234 whole leaf extracts does not differ significantly between *dgat3-2* and WT (**Fig. 4A-B**). However,  
235 isolated chloroplast TAG content is reduced by ~60% in *dgat3-2* compared to WT plants,  
236 confirming the role of *DGAT3* in plastidic TAG synthesis. Furthermore, the TAG TLC profile of  
237 isolated chloroplasts is enriched in TAGs with a higher Rf than those from whole leaves,  
238 overlapping the extra virgin olive oil standard (C18:1 74%, C18:2/3 11%, C16:0 15%).

239 Manipulation of plant lipid metabolism can result in altered defense signaling and  
240 response including elevated SA responses and/or cell death (Kachroo and Kachroo 2009) that  
241 restrict powdery mildew growth and reproduction (e.g. C. A. Frye and Innes 1998; Reuber et al.  
242 1998; Catherine A. Frye, Tang, and Innes 2001). Similar to WT, no cell death is observed in  
243 epidermal or mesophyll cells at the powdery mildew infection site of *dgat3-2* plants (**Fig. 4C**).  
244 Moreover, induced *PR-1* expression, a marker of SA-dependent defense responses, does not  
245 differ between WT and *dgat3-2* infected leaves (**Fig. 4D**). Together, these findings suggest the  
246 reduction in spore production observed for *dgat3-2* is due to decreased induced plastid TAG  
247 production, not increased defense.

### 248 **Powdery mildew infection induces the breakdown of thylakoid membrane lipids**

249 Above, we show powdery mildew-induced lipid bodies are associated with chloroplasts  
250 (**Fig. 3**) and plastid-localized AtDGAT3 is a dominant contributor to powdery mildew-induced  
251 host TAG synthesis and fungal spore production (**Figs. 2, 4**). As some stresses induce the  
252 accumulation of storage lipids at the expense of membrane lipids (Lu et al. 2020; Shiva et al.

253 2020), we postulated that host chloroplast membranes, dominated by thylakoid membranes, are  
254 being disassembled for TAG synthesis in response to infection. We therefore examined the  
255 abundance of thylakoid membrane lipids by electrospray ionization (ESI)-MS/MS. Uninfected  
256 mature *Arabidopsis* leaf thylakoid membrane lipids are dominated by  
257 monogalactosyldiacylglycerol (MGDG, 42%), digalactosyldiacylglycerol (DGDG, 13%), and  
258 phosphatidylglycerol (PG, 10%) (Browse et al. 1989). Powdery mildew-infected (washed) leaves  
259 extracted at 12 dpi show that MGDG, DGDG, and PG each decrease by at least 2-fold compared  
260 to uninfected leaf controls indicating the breakdown of thylakoid membranes (**Fig. 5A**,  
261 **Supplemental Dataset 2**). Decreased PG, by 60%, was also observed by LC-MS/MS (**Fig. 1H**).

262 To understand the change in total FA profiles, lipid extractions were performed on  
263 uninfected leaves, washed infected leaves and spore tissues at 12 dpi. Acyl chains were then  
264 converted to fatty acid methyl esters (FAMEs) for separation by gas chromatography with flame  
265 ionization detection (GC-FID). Principal component analysis (PCA) shows a distinct clustering  
266 of the three tissue types according to the ten FA species detected (**Fig. 5B**). Acyl chains  
267 associated with thylakoid membrane lipids, C18:3 (dominant), C18:2, and C16:3 (unique to  
268 chloroplast), each decrease by ~50% in 12 dpi leaves compared with uninfected (**Fig. 5C**). By  
269 contrast, the VLCFA C20:0 increases by ~20 fold in washed infected leaves. In spore extracts,  
270 the VLCFA C20:0 is the dominant species, followed by C18:3, while C18:3 dominates the leaf  
271 profiles even after the reduction shown with powdery mildew infection at 12 dpi. By normalizing  
272 the spore data to nmol/mgDW leaf (**Supplemental Dataset 2**), we can compare uninfected leaf  
273 total FA abundance with that of the washed leaves plus spores. We find 63% of total FA in the  
274 uninfected leaves is accounted for in the (washed) infected leaf plus spore (**Fig. 5D**). Moreover,  
275 only the spore C20:0 species abundance is clearly not fully attributed to leaf acquisition as the  
276 spore contains 2-fold more C20:0 than the (washed) infected leaf and 36-fold more C20:0 than  
277 the uninfected leaf on a leaf normalized basis (**Supplemental Dataset 2**). This also raises the  
278 possibility that some of the C20:0 in the (washed) infected leaf FAME samples and LC-MS/MS  
279 TAG samples (**Fig. 1, Supplemental Dataset 1**) may be fungal in origin. Only the fungal  
280 haustoria is present in the washed leaf samples as all surface structures are removed. Though  
281 haustoria make up a small percent of washed leaf sample cells on a cell basis, the haustoria are  
282 filled with lipid droplets (**Fig. 1**) that could include C20:0 remodeled by the fungus. Therefore, it  
283 is possible that a portion of the C20:0 in washed leaf analyses is fungal-derived.

284 As our findings above indicate thylakoid membrane breakdown occurs concurrent with  
285 TAG accumulation, we sought to specifically determine whether C16:3 FAs, unique to the  
286 thylakoid membrane (Browse et al. 1986), are present in TAGs from 12 dpi leaf lipid extracts  
287 (**Supplemental Dataset 1**). Five TAG species were identified as uniquely containing a C16:3  
288 acyl chain, and each of these TAGs also contains at least one C18:3 acyl chain. With infection,  
289 these C16:3 containing TAGs increase by 5.4-fold (**Fig. 5E**). Furthermore, the presence of C16:3  
290 FAs in spores (**Fig. 5C, Supplemental Dataset 2**) indicates fungal acquisition of these  
291 thylakoid-derived FAs.

292 We next sought to examine whether there is an associated change in chloroplast  
293 substructures with infection. We examined the ultrastructures of the powdery mildew haustorium  
294 and haustorium-associated chloroplasts at 5 dpi via transmission electron microscopy (TEM).  
295 The mature haustorium consists of a central haustorium body with peripheral small lobes (Koh et  
296 al. 2005). We see abundant electron-dense particles resembling lipid bodies in the haustorium  
297 body and lobes and in haustorium-associated chloroplasts (**Fig. 6A-C**). Examination of the  
298 haustorium-associated chloroplast in the epidermal cell shows an intact chloroplast outer  
299 membrane; however, the thylakoids have considerable loss of grana stacking, indicative of  
300 degradation (**Fig. 6D**).

301 Furthermore, the mesophyll chloroplast right underneath the haustorium shows severe  
302 degradation, with chloroplast envelope membrane and thylakoid membranes almost totally  
303 degraded (**Fig. 6E**) compared to mesophyll chloroplast from a parallel uninfected leaf  
304 (**Supplemental Figure S3**). In addition, no starch is present in this chloroplast. Because the  
305 thylakoid membranes are highly degraded in the infected sample, it is difficult to definitively  
306 ascertain whether these chloroplast lipid bodies are physically associated with the thylakoid  
307 membrane; however, at least one of the three, (**Fig. 6E**, LB-labeled lipid body), does not appear  
308 to be directly attached. Together, our data shows that concurrent with *G. orontii* asexual  
309 reproduction (5 dpi+), powdery mildew infection induces the breakdown of host thylakoids, as  
310 observed by TEM, with decreased whole leaf thylakoid galactolipids and thylakoid membrane  
311 lipid associated FAs.

312 **DISCUSSION**

313 **Powdery mildew- induced plastidic TAG synthesis utilizes the soluble metalloprotein**  
314 **DGAT3 to promote powdery mildew asexual reproduction**

315 **Figure 7** builds on the literature (Browse et al. 1986; Hözl and Dörmann 2019; C. Xu,  
316 Fan, and Shanklin 2020; Vanhercke et al. 2019; C. Xu and Shanklin 2016; Bates 2022) to  
317 integrate our findings into a simplified model that shows rewiring of host lipid metabolism by  
318 the powdery mildew for TAG synthesis at the expense of thylakoid membranes. In this study, we  
319 analyzed the changes in *Arabidopsis* leaf lipids in response to powdery mildew infection at  
320  $\geq$ 5dpi concurrent with the formation of spores replete with lipid bodies (**Fig. 1B**). Despite the  
321 highly localized induction of host lipid bodies in mesophyll cells underlying fungal feeding  
322 structures (**Fig. 3**), powdery mildew infected leaves show a 3.5-fold increase in TAG abundance  
323 at 12 dpi (**Fig. 1D**). Localized thylakoid unstacking and degradation (**Fig. 6**), decreased  
324 thylakoid lipids MGDG, DGDG, and PG (**Fig. 5A**) and decreased thylakoid membrane lipid FAs  
325 (**Fig. 5C**) all suggest TAGs are formed at the expense of thylakoid lipids. This is confirmed by  
326 the increase in TAGs containing thylakoid membrane derived acyl chains (18:3 dominant, 18:2,  
327 16:3 unique) (e.g. **Fig. 1G, 5E, Supplemental Dataset 1**) with infection.

328 We further find that the unusual DGAT enzyme, the soluble AtDGAT3 metalloprotein, is  
329 localized to the chloroplast (**Fig. 2C**) and responsible for the bulk (60%) of powdery mildew-  
330 induced TAG synthesis in the chloroplast (**Fig. 4A-B**). TLC shows TAGs from chloroplasts  
331 isolated from powdery mildew-infected leaves (**Fig. 4A-B**) are enriched in TAGs that run  
332 similarly to the extra virgin olive oil standard (85% C18 and 15% C16 FAs). This suggests that  
333 the chloroplast TAGs made via AtDGAT3 are enriched for thylakoid-derived acyl chains, as we  
334 observe in washed infected whole leaves (**Figs. 1G, 5E, Supplemental Dataset 1**). Furthermore,  
335 AtDGAT3 preferentially incorporates C18:3, the dominant FA in thylakoid membranes, and to a  
336 lesser extent C18:2 substrates into TAGs ([Hernández et al. 2012; Aymé et al. 2018](#)). It is unclear  
337 whether AtDGAT3 may utilize C16:3 as the experimental systems employed by (Hernández et  
338 al. 2012; Aymé et al. 2018) had little available C16:3. Powdery mildew spore production is  
339 significantly reduced when *AtDGAT3* expression is silenced or when a null mutant in *AtDGAT3*  
340 is assessed (**Fig. 2B**). This reduction in spore production is not associated with a pleiotropic  
341 phenotype, enhanced SA defense, and/or cell death in *dgat3-2*. (**Fig. 4C-D**). Therefore, it appears

342 that TAGs synthesized by DGAT3 in the chloroplast at the expense of thylakoid lipids promote  
343 powdery mildew asexual reproduction.

344 At 5 dpi, lipid bodies are observed directly under and in the haustorial complex and are  
345 mainly associated with chloroplasts (**Figs. 1C, 3, 6**). By 10 dpi, chloroplast-associated lipid body  
346 accumulation extends to neighboring mesophyll cells underneath the haustorial complex (**Fig. 3**).  
347 As indicated in our model (**Fig. 7**), 3D reconstructed confocal images suggest chloroplast lipid  
348 bodies may then be released into the cytosol for fungal acquisition, as the chloroplast lipid bodies  
349 embedded in the chloroplast, adjacent to the chloroplast, and in the cytosol are of similar size  
350 (**Fig. 3D**). It is possible that the induced chloroplast lipid bodies derive (in part) from  
351 plastoglobules as our TEM image indicates some lipid bodies in the chloroplast of the mesophyll  
352 cell adjacent to the haustorium to be directly associated with the thylakoid membrane (**Fig. 6**).  
353 However, at 5-6 um (**Fig. 3D**), the lipid bodies are at the top of the size range reported for stress-  
354 induced leaf plastoglobules (Arzac, Fernández-Marín, and García-Plazaola 2022; Bouchnak et al.  
355 2023), but common for cytosolic lipid droplets (C. Xu, Fan, and Shanklin 2020).

356 DGAT3 has not been identified in *Arabidopsis* plastoglobule proteomics datasets  
357 (Ytterberg, Peltier, and van Wijk 2006; Vidi et al. 2006; Lundquist et al. 2012; Espinoza-Corral,  
358 Schwenkert, and Lundquist 2021); however, stromal proteins have been identified in  
359 plastoglobule subpopulations that also contain thylakoid photosynthetic proteins and lipids but  
360 whose membrane varies in composition from that of thylakoid membranes (Ghosh et al. 1994;  
361 Smith, Licatalosi, and Thompson 2000). Moreover, plastoglobule blebbing into the stroma  
362 and/or release into the cytosol (Ghosh et al. 1994; Springer et al. 2016) has been implicated (C.  
363 Xu, Fan, and Shanklin 2020). If the powdery mildew-induced chloroplast lipid bodies derive (in  
364 part) from plastoglobules, they may contain the thylakoid membrane-bound phytol ester synthase  
365 1 (PES1) and/or PES2 (Ytterberg, Peltier, and van Wijk 2006; Vidi et al. 2006) which, in  
366 addition to phytol ester synthase activity, can synthesize TAGs via DAGs and acyl groups from  
367 acyl-CoA (preferred) (Lippold et al. 2012). As 40% of induced chloroplast TAGs remain in  
368 *dgat3-2* (**Fig. 4A**), it is tempting to speculate that in addition to DGAT3, PES1 and/or PES2 also  
369 contribute to powdery mildew-induced plastidic TAG synthesis.

370 How these TAGs directly benefit the powdery mildew remains to be determined. While  
371 plastidic TAG catabolism could serve as an immediate energy source, these storage lipids/lipid  
372 bodies could also be transported with or without fungal remodeling to the newly developing

373 spores which themselves are filled with lipid bodies containing TAGs (**Fig. 1B**). The presence of  
374 C16:3 acyl chains in spore lipids (**Fig. 5C, Supplemental Dataset 2**) indicates fungal acquisition  
375 of the chloroplast TAGs. These spore storage lipids then serve as an energy source to support  
376 spore germination and early colonization events prior to haustorium formation (Both et al. 2005).  
377 It is also possible that a host-derived lipid may be required for a fungal asexual reproductive  
378 signal. For example, in *Aspergillus nidulans* specific endogenous 18:2-derived oxylipins control  
379 sporulation versus sexual reproduction (Tsitsigiannis et al. 2004). In the arbuscular mycorrhizal  
380 fungi (AMF) - plant host symbiosis, plant derived C16:0 2-MGs are remodeled by the AMF  
381 fungus and act both as energy sources (immediate and stored as lipid bodies in spores) and as  
382 signals for fungal development, including sporulation (Kameoka et al. 2019). Plastoglobules  
383 often contain plant enzymes involved in oxylipin synthesis that could participate in the  
384 production of a fungal reproductive signal (Michel, Ponnala, and van Wijk 2021). This could be  
385 particularly important for obligate biotrophs such as powdery mildews characterized by missing  
386 or incomplete pathways for specialized metabolites as compared to other *Ascomycetes* including  
387 *A. nidulans* (Spanu 2012).

388 **ER-associated TAGs hinder powdery mildew asexual reproduction**

389 To our initial surprise, we found mutants that limit TAG accumulation in the ER exhibit  
390 increased powdery mildew spore production (**Fig. 2**). In Arabidopsis, DGAT1 is responsible for  
391 generating TAG from a rapidly produced pool of DAG derived from PC (Regmi et al. 2020). On  
392 the other hand, PDAT1 and DGAT2 are reported to use a different and larger pool of DAG,  
393 which has a relatively slower turnover (Regmi et al. 2020). Reduced *DGAT1* expression results  
394 in enhanced spore production (75% increase, **Fig. 2B**), while no difference is observed when  
395 *PDAT1* or *DGAT2* expression is perturbed (**Fig. 2A,B**). This suggests a rapidly produced pool of  
396 DAG from PC available to DGAT1 is used for powdery mildew-induced TAG production in the  
397 ER (**Fig. 7**). We further explored the impact of ABAC9 demonstrated to import FA/acyl-CoA  
398 into the ER and found the *abca9-1* mutant supports 50% increased powdery mildew spore  
399 production (**Fig. 2A**). By contrast, the long chain acyl-activating *lacs1-1* mutant, the only ER-  
400 localized LACS with enhanced expression at the powdery mildew infection site at 5 dpi  
401 (Chandran et al. 2010), did not alter powdery mildew spore production (**Fig. 2A**). Similarly, a  
402 mutant in ER-localized *LACS2* had no impact on powdery mildew growth and reproduction

403 (Tang, Simonich, and Innes 2007). As LACS1, LACS2, LACS4, and LACS8 are all ER-  
404 localized (Weng et al. 2010; Zhao et al. 2010; Jessen et al. 2015), it is likely that multiple ER  
405 LACS activate imported FAs.

406 Collectively, our findings indicate induced TAG biosynthesis in the ER via DGAT1  
407 impedes the asexual reproduction of powdery mildew (**Fig. 7**). AtDGAT1 acyl specificity differs  
408 from that of AtDGAT3. C16:0 is the preferred substrate of AtDGAT1, with little activity with  
409 C18:2 or C18:3 (Zhou et al. 2013; Aymé et al. 2014). C16:0 is a minor component of thylakoid  
410 membrane galactolipids (Browse et al. 1989; Mats X. Andersson, J. Magnus Kjellberg, and  
411 Sandelius 2001), consistent with AtDGAT1 use of precursor pools in the ER distinct from those  
412 used in the chloroplast by AtDGAT3.

413 How do ER-synthesized TAGs limit the growth of the biotrophic pathogen? TAGs  
414 synthesized at the ER membrane are typically packaged into organelles known as lipid droplets  
415 (LDs) that bud from the ER and accumulate in the cytosol (Guzha et al. 2023). Sequestration of  
416 these TAGs could be a means of nutrient restriction by the host if these LDs are not accessible to  
417 the powdery mildew. Furthermore, given DGAT3-dependent TAG synthesis in the chloroplast  
418 supports powdery mildew spore production, it is likely the competing pathway for TAG  
419 synthesis in the ER via DGAT1 may divert precursors from the chloroplast pathway (**Fig. 7**). For  
420 example, substrates for plastidic TAG synthesis may be limited by DGAT1 activity pulling  
421 plastidic FAs to the ER and/or reducing export of DAG/DAG precursors from the ER to the  
422 chloroplast. This competition has been observed in engineered tobacco leaves that accumulate oil  
423 at 15% of dry weight (Zhou et al. 2019) and reflects that TAG synthesis drives precursor flux  
424 (Bates and Browse 2012).

425 In addition, LDs not only contain TAGs and sterol esters, but may be sites of specialized  
426 biochemistry during stress (Shimada, Hayashi, and Hara-Nishimura 2017). Increased LDs have  
427 been observed in leaves infected by the hemi-biotrophic fungus *Colletotrichum higginsianum*  
428 and proposed to be sites of phytoalexin synthesis, preventing pathogen spread (Shimada et al.  
429 2014). Furthermore, LDs induced in response to avirulent *Pseudomonas syringae* infection of  
430 *Arabidopsis* leaves were found to contain camalexin biosynthetic enzymes (Fernández-Santos et  
431 al. 2020). Genes involved in indole-3-acetaldoxime derived phytoalexin production associated  
432 with defense against powdery mildews (Clay et al. 2009; Liu et al. 2016; Hunziker et al. 2020)  
433 exhibit enhanced expression at the powdery mildew infection site at 5 dpi (Chandran et al.

434 2010). This raises the possibility that increased synthesis and/or exposure to defensive  
435 specialized metabolites may contribute to the reduction in powdery mildew spore production  
436 associated with ER-derived LDs (**Fig. 7**).

437 **Powdery mildew infection offers valuable insights into the intricacy of plant lipid  
438 metabolism**

439 Although TAGs typically do not accumulate to significant levels in vegetative tissues,  
440 TAG accumulation in leaf tissue occurs in response to diverse environmental stresses and leaf  
441 senescence (Lu et al. 2020). While a role for AtDGAT3 has not been assessed in response to  
442 environmental stresses or leaf senescence, our study shows the important role AtDGAT3 plays in  
443 the powdery mildew-host interaction. This indicates AtDGAT3 function should be examined  
444 under other conditions, particularly those in which thylakoid disassembly is observed and  
445 induced TAGs are enriched in thylakoid-derived FAs, such as response to N limitation and  
446 senescence (Kaup, Froese, and Thompson 2002; Gaude et al. 2007; Besagni and Kessler 2013).  
447 Our work also argues for tracking cytosolic lipid droplet (LD) origins, as they were previously  
448 assumed to be ER-derived. And, the powdery mildew system provides a phenotype (impact on  
449 spore production) for distinguishing chloroplast-derived TAGs (via AtDGAT3) from those  
450 produced in the ER via AtDGAT1. Whether this translates to other (obligate) plant biotrophs of  
451 vegetative tissue remains to be investigated.

452 As shown by the root colonizing- obligate symbiont AMF, TAGs are only one possible  
453 source of lipids for microbial acquisition. AMF manipulate plant root cells to produce 2-MGs for  
454 fungal acquisition (Kameoka and Gutjahr 2022). In both systems, localized endoreduplication  
455 occurs and is associated with enhanced metabolic capacity that may allow for increased flux to  
456 FAs (Wildermuth 2010; Wildermuth et al. 2017). While AMF shifts lipid metabolism to 2-MG  
457 production through the use of enzymes specific to AMF host plants, the powdery mildew  
458 employs DGAT3, present in almost all land plants (Yan et al. 2018), for chloroplast TAG  
459 formation to support asexual reproduction (**Figs. 2, 4**). Therefore, specific host transporters may  
460 not be required as they are for AMF 2-MGs. Instead, lipid bodies that originate in the chloroplast  
461 have the potential to be directly acquired by the powdery mildew. Similarly, a number of human  
462 intracellular pathogens acquire host lipid bodies for their nutrition and development (Vallochi et  
463 al. 2018).

464 **DGAT3, a unique class of DGAT enzyme**

465 The three classes of *Arabidopsis* DGAT enzymes contain distinct conserved domains and  
466 have evolved independently in plants (Yin et al. 2022). The least studied class, DGAT3 enzymes,  
467 are unique in that they are soluble metalloproteins, with no transmembrane domain, and a  
468 thioredoxin-like ferredoxin domain containing a [2Fe-2S] cluster (Aymé et al. 2018). While  
469 AtDGAT3 (**Fig. 2C**) and *Paeonia rockii* PrDGAT3 (Han et al. 2022) are clearly localized to the  
470 chloroplast; other DGAT3 enzymes have been characterized as cytosolic (peanut, (Saha et al.  
471 2006); soybean, (Xue et al. 2022); *Camelina sativa*, (Gao et al. 2021)).

472 *AtDGAT3* is widely expressed at levels often 10-fold higher than *AtDGAT1* and  
473 *AtDGAT2*, with highest expression in the hypocotyl and mature and senescent leaf petioles and  
474 stems (Klepikova et al. 2016). Consistent with findings for powdery mildew infection of mature  
475 *Arabidopsis* leaves (Chandran et al. 2009, 2010), *AtDGAT3* is not strongly induced in response  
476 to pathogen or abiotic stress, assessed using the *Arabidopsis* eFP Browser (Winter et al. 2007).  
477 As changes in *AtDGAT3* expression are minimal, AtDGAT3 activity may depend on the  
478 availability of preferred precursors (e.g. released from thylakoid degradation). Furthermore,  
479 AtDGAT3 activity may be regulated by insertion of preformed [2Fe-2S] into the apoprotein in  
480 the plastid (Przybyla-Toscano et al. 2018) and by redox.

481 The availability of [2Fe-2S] clusters, along with maturation factors, could therefore  
482 impact DGAT3 metalloprotein levels. We found AtDGAT3 to participate in chloroplast TAG  
483 accumulation (**Fig. 4**) concurrent with thylakoid membrane degradation (**Figs. 5, 6**). When  
484 thylakoid membranes are broken down, as we observe in response to powdery mildew, [2Fe-2S]  
485 clusters released from thylakoid metalloproteins may be available for insertion into the  
486 AtDGAT3 apoprotein. The AtDGAT3 metalloprotein could then help minimize lipotoxicity by  
487 converting toxic free fatty acids and DAGs into storage lipids.

488 Redox state is also likely to regulate the activity of AtDGAT3. Chloroplast redox status,  
489 responsive to environmental cues, controls much of chloroplast function including lipid  
490 metabolism (Hernández and Cejudo 2021). Ayme et al. (2018) found the AtDGAT3 [2Fe-2S]2+  
491 cluster is stable, while the reduced [2Fe-2S]+ form of the enzyme is rapidly destroyed. When  
492 thylakoid membranes are disassembled and/or degraded, reductant generated from oxidative  
493 phosphorylation would be decreased and could be insufficient to reduce the AtDGAT3

494 metallocluster. Similarly, conditions resulting in plastidic oxidative stress (such as high light)  
495 could stabilize DGAT3, reducing lipotoxicity.

496 Engineered plants with increased TAG yield and low input costs for biofuel or  
497 specialized chemical applications (Pfleger, Gossing, and Nielsen 2015) could be designed to take  
498 advantage of AtDGAT3's production of TAGs at the expense of thylakoid membranes. The  
499 associated TAG profile would be enriched in C18:3 and C18:2 fatty acids desirable for human  
500 nutrition (Kumar, Sharma, and Upadhyaya 2016). As shown in **Figure 4**, the TAGs from isolated  
501 chloroplasts infected with powdery mildew appear similar to that of commercial extra virgin  
502 olive oil and to be largely attributed to synthesis via AtDGAT3. By contrast the TAGs from  
503 infected whole leaves are dominated by TAGs with reduced FA chain length, indicated by the  
504 lower Rf, that are likely synthesized in the ER via DGAT1, consistent with its preference for  
505 C16:0 (Aymé et al. 2014). Transient expression of *AtDGAT3* or *PrDGAT3* in *N. benthamiana*  
506 leaves increases TAG production by ~2-fold (Hernández et al. 2012; Han et al. 2022), compared  
507 to 7-8-fold increase with *AtDGAT1* transient expression (Hernández et al. 2012; Vanhercke et al.  
508 2013). Therefore, in engineered plants, increased flux to plastidic TAG synthesis might be  
509 further enhanced by reducing *DGAT1*. In addition, controls over DGAT3 activity and stability  
510 would need to be addressed.

511 Not only does the powdery mildew system allow us to uncover the role of AtDGAT3 in  
512 plastid TAG biosynthesis, but it can also be used to dissect key regulators driving flux towards  
513 plastid TAG synthesis and lipid body secretion. While the powdery mildew-induced shift in leaf  
514 lipid metabolism is highly localized, heavy infection could further increase induced TAG levels  
515 from the 3-fold induction observed with the low/moderate levels of infection that facilitate our  
516 molecular and microscopic studies. By understanding how mature photosynthetically active  
517 leaves switch their metabolism to break down thylakoids to make and secrete storage lipids,  
518 higher yields of plant oils could potentially be achieved, than from extracted seeds or fruit.  
519 Furthermore, plants suitable for oil production could be expanded and deforestation associated  
520 with palm oil plantations could potentially be reduced, facilitating more sustainable and  
521 environmentally benign production.

522 **METHODS**

523 **Plant lines, growth, and powdery mildew infection**

524 *Mutant list:* Seeds of *abca9-1* (SALK\_058070, Kim et al. 2013), *lacs1-1*  
525 (SALK\_127191, Lü et al. 2009), *dgat1-1* (CS3861, Katavic et al. 1995), *dgat3-2*  
526 (SALK\_112303, **Supplemental Fig. S2**), *pdat1-2* (SALK\_065334, Zhang et al. 2009) mutant  
527 lines in Col-0 background were obtained from Arabidopsis Biological Resource Center (ABRC)  
528 at The Ohio State University. All lines were genotyped to confirm homozygosity, using primers  
529 in **Supplemental Table S1**.

530 Wild type *Arabidopsis thaliana* ecotype Columbia-0 (Col-0) and mutants were grown in  
531 SS Metromix200 soil (Sun Gro, Bellevue, WA) in growth chambers at 22°C with 12 h light/dark  
532 cycle, 70% relative humidity and PAR of  $\sim 120 \mu\text{mol m}^{-2} \text{ s}^{-1}$ . After stratification at 4°C,  
533 alternating Col-0 and mutant seeds were planted in 16.5 cm insert boxes (12 plants/box; 6  
534 boxes/flat). For whole plant spore count phenotyping, boxes of plants were inoculated at 4 weeks  
535 by settling tower with a moderate dose of 10-14 dpi conidia from *G. orontii* MGH1 at consistent  
536 time of day (Reuber et al. 1998).

537 **Spray-induced gene silencing (SIGS)**

538 SIGS protocol was adapted from McRae *et.al.* (2023) (McRae et al. 2023). pssRNAit  
539 (<https://plantgrn.noble.org/pssRNAit/>) was used to design an efficient and specific dsRNA for  
540 *DGAT1* (AT2G19450), *DGAT2* (AT3G49210), and *DGAT3* (AT1G48300). Templates were  
541 amplified (primers in **Supplemental Table S1**) from Col-0 cDNA and prepared for *in vitro*  
542 transcription with the HiScribe T7 High Yield RNA Synthesis Kit (New England Biolabs,  
543 Ipswich, MA). After purification with Monarch RNA Cleanup Kit (New England Biolabs,  
544 Ipswich, MA), RNA was reannealed, quantified and aliquoted in nuclease-free water. 12-15  
545 mature fully expanded Arabidopsis leaves from 4-5 4-week old plants were harvested. Petioles  
546 were inserted through a Whatman 1.0 paper overlaid into 1/2 MS salts (Research Products  
547 International, Prospect, IL), 0.1% 2-(N- morpholino)ethanesulfonic acid (Merck Millipore,  
548 Burlington, MA), and 0.8% agar (BD Biosciences, San Jose, CA) in 150 mm plates. Paired  
549 plates (with mutant and WT leaves) were placed under the settling tower and infected with 10-14

550 dpi conidia, as above. 40µg RNA (or nuclease-free mock) was sprayed at 1 hpi and 2 dpi.

551 **Spore tissue collection and counting**

552 Powdery mildew spore production/mg leaf fresh weight protocol was adapted from  
553 Weßling and Panstruga (Weßling and Panstruga 2012). Briefly, at 8-10 dpi, leaves 7-9 from WT  
554 and mutant plants in a box, or all 12 leaves from mock and dsRNA- treated plates, were  
555 harvested. Spores were washed off leaves by vortexing in 15 mL 0.01% Tween-80 for 30  
556 seconds and filtered through 30µm CellTrics filter (Sysmex America, Lincolnshire, IL) before  
557 centrifugation at 4000xg. The resulting spore pellet was resuspended in 200-1000µL water. For  
558 each sample, nine 1 × 1 mm fields of a Neubauer-improved haemocytometer were counted. For  
559 lipid analysis, tissue was immediately frozen and stored until extraction. For spore counting, 3  
560 paired counts of WT and mutant spore suspensions from a box were performed on a Neubauer-  
561 improved hemocytometer (Hausser Scientific, Horsham, PA). Spore counts were divided by the  
562 fresh weight of the plant tissue to determine spores/mgFW, and then normalized to WT counts.  
563 To determine significance, an unpaired, two-tailed Student's T-test was performed on counts  
564 from at least 5 boxes ( $p < 0.05$ ).

565 **Trypan blue staining**

566 To visualize cell death, leaf tissues were incubated for 16 h at 24°C in the staining  
567 solution (2.5 mg/ml trypan blue in lactophenol, lactic acid, glycerol, phenol, water (1:1:1:1)), and  
568 two volumes of ethanol were added to this solution. The tissues were cleared in chloral hydrate  
569 solution (2.5g/ml chloral hydrate in water) for 16 h at 24°C. Leaf tissues were transferred to 70%  
570 glycerol and viewed using the AS Laser Microdissection system microscope (Leica  
571 Microsystems, Deerfield, IL). Note that trypan blue also slightly stains fungal structures.

572 **Reverse transcription (RT)-qPCR analysis**

573 Total RNA from leaves was extracted with RNA using Spectrum (Sigma-Aldrich) Plant  
574 Total RNA Kit according to the manufacturer's protocol. Residual genomic DNA was digested  
575 with DNase I (DNaseI, Qiagen). PCR was performed using cDNA using High-Capacity cDNA  
576 Reverse Transcription Kit (ThermoFisher Scientific). The gene specific primers for DGAT3 are:  
577 P1: 5'-ACCAGAACGGTAGGGTTCG-3'; P2: 5'-CTAACGTTGGGCCATCACGAC-3'.

578 Amplification was performed using the following conditions: 95°C for 2 min and 30 cycles of  
579 95°C for 30 s, 60°C for 30 s, and 72°C for 90 s.

580 To analyze the expression levels of *PR1* in *dgat3-2* and Col-0 with powdery mildew  
581 infection, three independently grown biological replicates of two fully expanded leaves (leaves  
582 7-9) at 5 dpi were used for comparison. Tissue was immediately frozen in liquid nitrogen and  
583 stored at -80°C until extraction. RNA was extracted using Spectrum (Sigma-Aldrich) Plant Total  
584 RNA Kit according to the manufacturer's protocol. Residual genomic DNA was digested with  
585 DNase I (DNaseI, Qiagen). Purity and concentration of RNA was confirmed with Nanodrop-  
586 1000 spectrophotometer (ThermoFisher Scientific). Complementary DNA (cDNA) was  
587 synthesized from 1µg RNA using High-Capacity cDNA Reverse Transcription Kit  
588 (ThermoFisher Scientific). Quantitative real-time PCR (qPCR) experiments were performed in a  
589 BioRad CFX96 (BioRad) using the iTaq Universal SYBR Green Supermix (Bio-Rad, USA),  
590 following kit instructions. For all genes, thermal cycling started with a 95°C denaturation step  
591 for 10 min followed by 40 cycles of denaturation at 95°C for 15 s and annealing at 56°C for 30 s.  
592 Each run was finished with melt curve analysis to confirm specificity of amplicon. Three  
593 technical replicates were performed for each experimental set. Gene expression (fold change)  
594 was calculated normalized to ACTIN2 (At3g18780) as reference gene, and calculated using the  
595 Do My qPCR Calculations webtool ([http://umrh-bioinfo.clermont.inrae.fr/do\\_my\\_qPCRcalc/](http://umrh-bioinfo.clermont.inrae.fr/do_my_qPCRcalc/);  
596 (Tournayre et al. 2019). Primer sequences are provided in **Supplemental Table S1**.

597 **Golden Gate cloning and transient expression of DGAT3 via Agrobacterium infiltration**

598 The full-length genomic DNA encoding *DGAT3* (*AT1G48300*) without stop codon and  
599 with removal of an internal restriction site for BsaI was utilized. Two BsaI restriction enzyme  
600 sites are added to both 5' and 3' end of sequence using PCR primers listed in **Supplemental**  
601 **Table S1**. The sequence was cloned into pICSL22010 plasmid (with C-terminal GFP and CaMV  
602 35S promoter) by Golden Gate cloning. The vector was transformed into *Agrobacterium*  
603 *tumefaciens* GV3101. *A. tumefaciens* transformants were grown in 5 mL liquid LB with  
604 appropriate antibiotics overnight at 28°C, pelleted, resuspended in induction media (10 mM  
605 MES pH 5.6, 10 mM MgCl<sub>2</sub>, 150 µM acetosyringone) to an OD600 of 0.4-0.60 for transient  
606 expression, and incubated in induction media for approximately 3-4 h before infiltration in *N.*

607 *benthamiana* leaves. GFP fluorescence was observed at 48-72 hpi by Zeiss LSM710 confocal  
608 microscope (Carl Zeiss Inc, White Plains, New York) at the RCNR Biological Imaging Facility,  
609 UC Berkeley.

610 **Confocal imaging**

611 Confocal scanning fluorescence microscopy with a Zeiss LSM710 confocal microscope  
612 (Carl Zeiss Inc, White Plains, New York) at the RCNR Biological Imaging Facility, UC  
613 Berkeley was utilized to examine fungal haustoria and lipid droplets.

614 Col-0 lines expressing RPW8.2-YFP under the native promoter were inoculated with *G.*  
615 *orontii* to visualize fungal haustoria (W. Wang et al. 2009). The 3D reconstruction of RPW8.2-  
616 YFP was performed using Imaris software. To visualize lipid bodies, tissues were stained with  
617 0.004 mg/mL BODIPY 505/515 and vacuum infiltrated for 10 min before imaging. Excitation of  
618 chlorophyll and BODIPY were at 633 and 488 nm, respectively. Emission wavelength for  
619 chlorophyll and BODIPY-stained lipid bodies was 647-721 nm and 493-589 nm, respectively.  
620 Percent-area of BODIPY fluorescence was quantified using Image J software. The 3D  
621 reconstruction of lipid droplets and chloroplasts was performed using Imaris.

622 **Transmission electron microscopy imaging**

623 Arabidopsis Col-0 4 week old plants were heavily inoculated with *G. orontii*. Leaves  
624 were sampled at 5 dpi and cut into 2 × 3-mm sections, fixed in buffer containing 2.5%  
625 glutaraldehyde, 2% tween 20, 0.05M sodium cacodylate and 4% formaldehyde in microwave for  
626 2 X 40 s. The fixed tissues were vacuumed for 1 h or as long as possible until they sank to the  
627 bottom. The tissues were rinsed three times in 0.05M sodium cacodylate buffer for 10 min. After  
628 being transferred into 1% Osmium tetroxide buffer, the tissues were fixed by microwaving for 3  
629 X 1 min, with 15 min vacuum between each microwaving. The samples were dehydrated with a  
630 gradient of acetone (35%, 50%, 70%, 80%, 95%, 100%, 100%, 100%) for 10 min each. The  
631 tissues were sequentially infiltrated with 20%, 40%, 60% Resin by microwaving (3 min) and  
632 rotated overhead for 1 h after each microwaving. The samples were rotated in 80% resin for 16  
633 h. The next day, the samples were rotated in 90% resin 16 h. The samples were embedded in a  
634 flat embedding mold and cured in a 60°C oven for 2-3 days. Ultrathin sections were put on mesh  
635 nickel grids. After contrast staining, samples were examined and images were acquired with a

636 FEI Tecnai T12 Transmission Electron Microscope at the UC Berkeley Electron Microscopy  
637 Laboratory.

638 **TAGs and Phospholipids via LC-MS/MS**

639 Leaf tissue (leaves 7-9) was harvested at 12 dpi, rapidly weighed, and flash frozen until  
640 ready for extraction. After tissue disruption in the bead beater, modified Bligh & Dyer extraction  
641 with methanol:chloroform:H<sub>2</sub>O (1:1:0.9) was performed, 300 µL of chloroform phase was  
642 recovered, and dried under nitrogen. The dried extracts were resuspended in 200µL of  
643 Isopropanol (IPA):Acetonitrile (ACN):Methanol (MeOH) (3:3:4), and run immediately. Internal  
644 standard mixes were used to ensure retention time reproducibility. Samples were run on an  
645 Agilent 1290 (Agilent Technologies, Santa Clara, CA) UHPLC connected to a QExactive mass  
646 spectrometer (Thermo Fisher Scientific, San Jose, CA) at the DOE Lawrence Berkeley Lab with  
647 the following chromatographic method, in both positive and negative mode. Source settings on  
648 the MS included auxiliary gas flow of 20 (au), sheath gas flow rate of 55 (au), sweep gas flow of  
649 2 (au), spray voltage of 3 kV (positive and negative ionization modes), and ion transfer tube  
650 temperature of 400 °C.

651 Lipids were run on a reversed phase 50mm x 2.1 mm, 1.8 µm Zorbax RRHD (Rapid  
652 Resolution High Definition) C18 column (Agilent Technologies) with a 21 min gradient and 0.4  
653 mL/min flow rate, with 2 µL injections. The mobile phases used were A: 60:40 H<sub>2</sub>O:ACN  
654 (60:40) with 5mM ammonium acetate, 0.1% formic acid, and B: IPA:ACN (90:10) with 5mM  
655 ammonium acetate (0.2% H<sub>2</sub>O), 0.1% formic acid. The system was held at 20% B for 1.5 min,  
656 followed by an increase to 55% B over 2.5 min, and a subsequent increase to 80% B over 6 min.  
657 The system was then held at 80% B for 2 min, before being flushed out with 100% B for 5 min,  
658 and re-equilibrated at 20% B over 5 min. The QExactive parameters were as follows: MS  
659 resolution was set to 70,000, and data was collected in centroid mode from 80-1200 m/z. MS/MS  
660 data was collected at a resolution of 17,500 with a collision energy step gradient of 10, 20, and  
661 30. Lipids were identified by comparing detected vs. theoretical lipid m/z and MS/MS  
662 fragmentation patterns, with lipid class and fatty acid composition determined based on  
663 characteristic product ions or neutral losses (see **Supplementary Dataset 1**). TAGs were  
664 detected in positive ionization mode as [M+NH<sub>4</sub>]<sup>+</sup> adducts, with FA tails determined by neutral

665 loss of ions detected in MS/MS fragmentation spectra. Phospholipids PC, lysoPC, PE, PI, and  
666 PG were detected in positive ionization mode as [M+H]<sup>+</sup> adducts, with PCs and lysoPCs having  
667 a characteristic product ion of 184, PEs a neutral loss of 141, PIs a neutral loss of 260 and PGs a  
668 neutral loss of 172 (Murphy 2014). Metabolomics raw data is deposited in the MassIVE data  
669 repository (<https://massive.ucsd.edu/>), accession number MSV000093317  
670 (doi:10.25345/C5N873941). Only lipid classes that have peak heights above the upper bound of  
671 the 95% confidence interval of the negative controls are included in **Supplemental Dataset 1** for  
672 further analysis.

673 **Thylakoid Membrane Lipid Analysis**

674 *Tissue harvest and lipid extraction:* Leaves 7-9 were harvested from mock infected and  
675 infected plants, washed of spores, frozen in liquid nitrogen, and stored at -80°C until extraction.  
676 Extraction was performed following lipase inactivation in 75°C isopropanol for 15 min  
677 according to (Devaiah et al. 2006) and electrospray ionization tandem mass spectrometry was  
678 performed at the Kansas Lipidomics Research Center Analytical Laboratory (Manhattan, KS) as  
679 below.

680 *Electrospray Ionization Tandem Mass Spectrometry Conditions:* The samples were  
681 dissolved in 1 ml chloroform. An aliquot of 10 to 20 $\mu$ l of extract in chloroform was used. Precise  
682 amounts of internal standards, obtained and quantified as previously described (Welti et al.  
683 2002), were added in the following quantities (with some small variation in amounts in different  
684 batches of internal standards): 0.36 nmol di14:0-PG, 0.36 nmol di24:1-PG, 0.36 nmol 14:0-  
685 lysoPG, 0.36 nmol 18:0- lysoPG, 2.01 nmol 16:0-18:0-MGDG, 0.39 nmol di18:0- MGDG, 0.49  
686 nmol 16:0-18:0-DGDG, and 0.71 nmol di18:0-DGDG. Samples were combined with solvents,  
687 introduced by continuous infusion into the ESI source on a triple quadrupole MS/MS (API 4000,  
688 Applied Biosystems, Foster City, CA), and neutral loss scans were acquired as described by  
689 (Shiva et al. 2013).

690 The background of each spectrum was subtracted, the data were smoothed, and peak  
691 areas integrated using a custom script and Applied Biosystems Analyst software. Peaks  
692 corresponding to the target lipids in these spectra were identified and the intensities corrected for  
693 isotopic overlap. Lipids in each class were quantified in comparison to the two internal standards

694 of that class. The first and typically every 11th set of mass spectra were acquired on the internal  
695 standard mixture only. A correction for the reduced response of the mass spectrometer to the  
696 galactolipid standards in comparison to its response to the unsaturated leaf galactolipids was  
697 applied. To correct for chemical or instrumental noise in the samples, the molar amount of each  
698 lipid metabolite detected in the “internal standards only” spectra was subtracted from the molar  
699 amount of each metabolite calculated in each set of sample spectra. Finally, the data were  
700 corrected for the fraction of the sample analyzed and normalized to the sample leaf dry weight  
701 (DW) to produce data in the units nmol/mg DW.

702 **FAME analysis**

703 Leaves 7-9 were harvested from mock infected and infected plants, washed of spores,  
704 frozen in liquid nitrogen, and stored at -80°C until extraction. Extraction was performed  
705 following lipase inactivation in 75°C isopropanol for 15 min according to (Devaiah et al. 2006)  
706 and FAME analysis was performed by the Kansas Lipidomics Research Center Analytical  
707 Laboratory (Manhattan, KS) as below.

708 Total lipid extracts were spiked with 25 nmol pentadecanoic (C15:0) acid as internal  
709 standard. Samples were evaporated under a stream of nitrogen. Samples were resuspended in 1  
710 mL 3 M methanolic hydrochloric acid and heated at 78°C for 30 min. Two mL H<sub>2</sub>O and 2 mL  
711 hexane were added followed by three hexane extractions and then dried down under a stream of  
712 nitrogen. Samples were then redissolved in 100 µL hexane and analyzed on GC-FID (Agilent  
713 6890N) after separating sample using a DB-23 capillary column (column length, 60 m; internal  
714 diameter, 250 µm; film thickness, 0.25 µm). The carrier was helium gas at a flow rate of 1.5  
715 mL/min. The back inlet was operating at a pressure of 36.01 psi and temperature of 250 °C. The  
716 GC oven temperature ramp began with an initial temperature of 150 °C held for 1 min and  
717 increased at 25 °C/min to 175 °C. Then the temperature was increased at 4 °C/min to 230°C and  
718 held at 230°C for 8 min. The total run time was 23.75 min. The flame ionization detector was  
719 operated at 260 °C. The hydrogen flow to the detector was 30 mL/min, air flow was 400 mL/min  
720 and sampling rate of the FID was 20 Hz. The data were processed using Agilent Chemstation  
721 software. As for above, only data with CoV < 0.3 were included. Data are presented as nmol/mg  
722 DW of the tissue utilized. Spore nmol/mg DW was multiplied by 0.12995 to indicate the

723 corresponding leaf mg/DW from which the spores were obtained.

724 **TLC of lipids from isolated chloroplasts and whole leaves**

725 Chloroplast isolation: Leaf tissue from about 40 *Arabidopsis* plants, infected with *G.*  
726 *orontii* MGH1 at 4-weeks, was harvested at 12 dpi and immediately homogenized by blending  
727 for 3x5 s in isolation buffer (30 mM HEPES-KOH pH 8, 0.33M sorbitol, 5 mM MgCl<sub>2</sub>, 0.1 %  
728 [w/v] BSA). The resulting homogenate was briefly filtered through one layer of Miracloth  
729 (Chicopee Mills Inc., Milltown, N. J.) Chloroplasts were pelleted with 5-min centrifugation at  
730 1500 g and 4°C, and washed twice with washing buffer (30 mM HEPES-KOH pH 8.0, 0.33M  
731 sorbitol). Washed chloroplasts were normalized by chlorophyll concentration and resuspended in  
732 an osmotic stress buffer (10 mM Tricine pH 7.9, 1 mM EDTA, 0.6 M sucrose) and stored at  
733 -80°C for future analysis.

734 1-3 mg chloroplasts (normalized by chlorophyll concentrations) or 1-2 g grounded whole  
735 leaf tissues from 4-5 week old plants (normalized by fresh weight) for infected samples at 12 dpi  
736 were sonicated with 4 pulses of 10 sec and 20% wattage (Model VCX 130, Sonics & Materials  
737 INC, Newtown, CT). 1 mL of 2:1 Chloroform Methanol (v/v) with 0.01% BHT was added and  
738 placed on a vortex for 5 min. 266 µL of 0.73% (w/v) NaCl solution was added, and the mixture  
739 was inverted 5-6 times to mix. Samples were then centrifuged for 5 min at 10,000 × g. The lower,  
740 solvent phase was used and dried under an N<sub>2</sub> stream and resuspended in 20 µL chloroform. In  
741 total, 10 µL of the concentrated lipid extract was loaded onto a clean silica TLC plate  
742 (MilliporeSigma™ TLC Silica Gel 60 F254: 25 Glass plates, M1057150001) and developed  
743 hexane:diethyl ether:glacial acetic acid (91:39:1.3) for 30 min. Lipids were visualized by sulfuric  
744 acid spray and charring (25% H<sub>2</sub>SO<sub>4</sub> in 50% ethanol, 135 °C for 10 min). Trader Giotto's extra  
745 virgin olive oil (0.01ug loaded) was used as a standard. TLC was conducted for four separate  
746 experiments, each serving as a biological replicate. Relative TAG content analysis was  
747 performed using ImageJ software.

748

749 **ACCESSION NUMBERS**

750 *ABCA9* (AT5G61730), *LACS1* (AT2G47240), *PDAT1* (AT5G13640), *DGAT1* (AT2G19450),  
751 *DGAT2* (AT3G51520), *DGAT3* (AT1G48300), *PR1* (At2g14610), MassIVE data repository  
752 (<https://massive.ucsd.edu/>) accession number MSV000093317.

753

754

755 **SUPPLEMENTAL MATERIALS**

756 **Supplemental Table S1.** Genotyping, cloning, and SIGS dsRNA template primers used for this  
757 work.

758 **Supplemental Figure S1.** Abundance of TAG species detected in infected leaves at 12 dpi,  
759 compared to uninfected leaves.

760 **Supplemental Figure S2.** Identification of *dgat3-2* (SALK\_112303) mutant.

761 **Supplemental Figure S3.** Transmission electron microscopy image of mesophyll chloroplast  
762 from uninfected *Arabidopsis* leaf.

763 **Supplemental Dataset 1: LC-MS/MS analysis.**

764 **Supplemental Dataset 2: FAME and ESI-MS/MS analysis.**

765

766 **ACKNOWLEDGEMENT**

767 This work was supported by National Science Foundation (NSF) MCB-1617020 and PFI-  
768 1919244, and USDA National Institute of Food and Agriculture, Hatch Project Accession  
769 Number 1016994 awards to MCW. HX also received a NRAEF Viticulture and Enology  
770 Scholarship. JS was supported through NSF MCB-1617020, with TN as co-PI. KL  
771 acknowledges support from the US Department of Energy Joint Genome Institute  
772 (<https://ror.org/04xm1d337>; operated under Contract No. DE-AC02-05CH11231 to Lawrence  
773 Berkeley National Laboratory). We thank Dr. Denise Schichnes at the RCNR Biological Imaging  
774 Facility and the staff of the Electron Microscope Laboratory at the University of California

775 Berkeley for their assistance. Microscopy imaging reported in this publication was supported in  
776 part by the National Institutes of Health S10 program under award number 1S10RR026866-01.  
777 The thylakoid lipid and FAME analyses described in this work were performed at the Kansas  
778 Lipidomics Research Center Analytical Laboratory (Manhattan, KS) by Mary Roth and Libin  
779 Yao. Instrument acquisition and lipidomics method development were supported by the National  
780 Science Foundation (including support from the Major Research Instrumentation program; most  
781 recent award DBI-1726527), K-IDeA Networks of Biomedical Research Excellence (INBRE) of  
782 National Institute of Health (P20GM103418), USDA National Institute of Food and Agriculture  
783 (Hatch/Multi-State project 1013013), and Kansas State University. We thank Dr. Shunyuan Xiao  
784 (University of Maryland, College Park) for RPW8-YFP Arabidopsis seeds, Dr. Ksenia Krasileva  
785 (UC Berkeley) for plasmid pICSL22010, and Dr. Krishna Niyogi (UC Berkeley) and Dr. Peter  
786 Dörmann (University of Bonn, Germany) for critical review of the manuscript.  
787

## 788 AUTHOR CONTRIBUTIONS

789 JJ, HX and MCW planned and designed the research. Spore counting of mutant and WT plants  
790 was performed by JJ and RM. JJ prepared samples for lipid analyses. HX performed DGAT3  
791 cloning and characterization. Confocal imaging was done by HX, and TEM by HX and JJ. JS,  
792 KL, and TN performed the LC-MS/MS TAG and PL analyses. JJ, HX and MCW wrote the  
793 manuscript. All authors contributed to the reviewing of the manuscript.

794

## 795 REFERENCES

796 Abood, J. K., and Dorothy M. Lösel. 1989. "Effects of Powdery Mildew Infection on the Lipid  
797 Metabolism of Cucumber." In *Biological Role of Plant Lipids*, edited by Péter A. Biacs,  
798 Katalin Gruiz, and Tibor Kremmer, 597–601. Boston, MA: Springer US.  
799 Arzac, Miren I., Beatriz Fernández-Marín, and José I. García-Plazaola. 2022. "More than Just  
800 Lipid Balls: Quantitative Analysis of Plastoglobule Attributes and Their Stress-Related  
801 Responses." *Planta* 255 (3): 62.  
802 Atella, Georgia C., Paula R. Bittencourt-Cunha, Rodrigo D. Nunes, Mohammed Shahabuddin,  
803 and Mário A. C. Silva-Neto. 2009. "The Major Insect Lipoprotein Is a Lipid Source to  
804 Mosquito Stages of Malaria Parasite." *Acta Tropica* 109 (2): 159–62.  
805 Aymé, Laure, Simon Arragain, Michel Canonge, Sébastien Baud, Nadia Touati, Ornella Bimai,  
806 Franjo Jagic, et al. 2018. "Arabidopsis Thaliana DGAT3 Is a [2Fe-2S] Protein Involved in  
807 TAG Biosynthesis." *Scientific Reports* 8 (1): 1–10.

808 Aymé, Laure, Sébastien Baud, Bertrand Dubreucq, Florent Joffre, and Thierry Chardot. 2014.  
809     “Function and Localization of the *Arabidopsis* Thaliana Diacylglycerol Acyltransferase  
810     DGAT2 Expressed in Yeast.” *PloS One* 9 (3): e92237.

811 Bates, Philip D. 2022. “Chapter Six - The Plant Lipid Metabolic Network for Assembly of  
812     Diverse Triacylglycerol Molecular Species.” In *Advances in Botanical Research*, edited by  
813     Fabrice Rébeillé and Eric Maréchal, 101:225–52. Academic Press.

814 Bates, Philip D., and John Browse. 2012. “The Significance of Different Diacylglycerol Synthesis  
815     Pathways on Plant Oil Composition and Bioengineering.” *Frontiers in Plant Science* 3  
816     (July): 147.

817 Baud, Sébastien, Bertrand Dubreucq, Martine Miquel, Christine Rochat, and Loïc Lepiniec.  
818     2008. “Storage Reserve Accumulation in *Arabidopsis*: Metabolic and Developmental  
819     Control of Seed Filling.” *The Arabidopsis Book / American Society of Plant Biologists* 6  
820     (July): e0113.

821 Besagni, Céline, and Felix Kessler. 2013. “A Mechanism Implicating Plastoglobules in  
822     Thylakoid Disassembly during Senescence and Nitrogen Starvation.” *Planta* 237 (2): 463–  
823     70.

824 Both, Maike, Michael Csukai, Michael P. H. Stumpf, and Pietro D. Spanu. 2005. “Gene  
825     Expression Profiles of *Blumeria Graminis* Indicate Dynamic Changes to Primary  
826     Metabolism during Development of an Obligate Biotrophic Pathogen.” *The Plant Cell* 17  
827     (7): 2107–22.

828 Bouchnak, Imen, Denis Coulon, Vincent Salis, Sabine D’Andréa, and Claire Bréhélin. 2023.  
829     “Lipid Droplets Are Versatile Organelles Involved in Plant Development and Plant  
830     Response to Environmental Changes.” *Frontiers in Plant Science* 14 (June): 1193905.

831 Browse, J., L. Kunst, S. Anderson, S. Hugly, and C. Somerville. 1989. “A Mutant of *Arabidopsis*  
832     Deficient in the Chloroplast 16:1/18:1 Desaturase.” *Plant Physiology* 90 (2): 522–29.

833 Browse, J., N. Warwick, C. R. Somerville, and C. R. Slack. 1986. “Fluxes through the  
834     Prokaryotic and Eukaryotic Pathways of Lipid Synthesis in the ‘16:3’ Plant *Arabidopsis*  
835     Thaliana.” *Biochemical Journal* 235 (1): 25–31.

836 Cavaco, Ana Rita, Ana Rita Matos, and Andreia Figueiredo. 2021. “Speaking the Language of  
837     Lipids: The Cross-Talk between Plants and Pathogens in Defence and Disease.” *Cellular  
838     and Molecular Life Sciences: CMS* 78 (9): 4399–4415.

839 Chandran, Divya, Noriko Inada, Greg Hather, Christiane K. Kleindt, and Mary C. Wildermuth.  
840     2010. “Laser Microdissection of *Arabidopsis* Cells at the Powdery Mildew Infection Site  
841     Reveals Site-Specific Processes and Regulators.” *Proceedings of the National Academy of  
842     Sciences of the United States of America* 107 (1): 460–65.

843 Chandran, Divya, Yu Chuan Tai, Gregory Hather, Julia Dewdney, Carine Denoux, Diane G.  
844     Burgess, Frederick M. Ausubel, Terence P. Speed, and Mary C. Wildermuth. 2009.  
845     “Temporal Global Expression Data Reveal Known and Novel Salicylate-Impacted Processes  
846     and Regulators Mediating Powdery Mildew Growth and Reproduction on *Arabidopsis*.”  
847     *Plant Physiology* 149 (3): 1435–51.

848 Clark, Joanna I. M., and J. L. Hall. 1998. “Solute Transport into Healthy and Powdery Mildew-  
849     Infected Leaves of Pea and Uptake by Powdery Mildew Mycelium.” *The New Phytologist*  
850     140 (2): 261–69.

851 Clay, Nicole K., Adewale M. Adio, Carine Denoux, Georg Jander, and Frederick M. Ausubel.  
852     2009. “Glucosinolate Metabolites Required for an *Arabidopsis* Innate Immune Response.”  
853     *Science* 323 (5910): 95–101.

854 Costa, G., M. Gildenhard, M. Eldering, R. L. Lindquist, A. E. Hauser, R. Sauerwein, C.  
855 Goosmann, V. Brinkmann, P. Carrillo-Bustamante, and E. A. Levashina. 2018. “Non-  
856 Competitive Resource Exploitation within Mosquito Shapes within-Host Malaria Infectivity  
857 and Virulence.” *Nature Communications* 9 (1): 1–11.

858 Dahlqvist, Anders, Ulf Ståhl, Marit Lenman, Antoni Banas, Michael Lee, Line Sandager, Hans  
859 Ronne, and Sten Stymne. 2000. “Phospholipid:diacylglycerol Acyltransferase: An Enzyme  
860 That Catalyzes the Acyl-CoA-Independent Formation of Triacylglycerol in Yeast and  
861 Plants.” *Proceedings of the National Academy of Sciences* 97 (12): 6487–92.

862 Devaiah, Shivakumar Pattada, Mary R. Roth, Ethan Baughman, Maoyin Li, Pamela Tamura,  
863 Richard Jeannotte, Ruth Welti, and Xuemin Wang. 2006. “Quantitative Profiling of Polar  
864 Glycerolipid Species from Organs of Wild-Type Arabidopsis and a Phospholipase D $\alpha$ 1  
865 Knockout Mutant.” *Phytochemistry* 67 (17): 1907–24.

866 Espinoza-Corral, Roberto, Serena Schwenkert, and Peter K. Lundquist. 2021. “Molecular  
867 Changes of Arabidopsis Thaliana Plastoglobules Facilitate Thylakoid Membrane  
868 Remodeling under High Light Stress.” *The Plant Journal: For Cell and Molecular Biology*  
869 106 (6): 1571–87.

870 Fan, Jilian, Chengshi Yan, and Changcheng Xu. 2013. “Phospholipid:diacylglycerol  
871 Acyltransferase-Mediated Triacylglycerol Biosynthesis Is Crucial for Protection against  
872 Fatty Acid-Induced Cell Death in Growing Tissues of Arabidopsis.” *The Plant Journal: For  
873 Cell and Molecular Biology* 76 (6): 930–42.

874 Fernández-Santos, Rubén, Yovanny Izquierdo, Ana López, Luis Muñiz, Marta Martínez, Tomás  
875 Cascón, Mats Hamberg, and Carmen Castresana. 2020. “Protein Profiles of Lipid Droplets  
876 during the Hypersensitive Defense Response of Arabidopsis against Pseudomonas  
877 Infection.” *Plant & Cell Physiology* 61 (6): 1144–57.

878 Fotopoulos, Vasileios, Martin J. Gilbert, Jon K. Pittman, Alison C. Marvier, Aram J. Buchanan,  
879 Norbert Sauer, J. L. Hall, and Lorraine E. Williams. 2003. “The Monosaccharide  
880 Transporter Gene, AtSTP4, and the Cell-Wall Invertase, Atbetafruct1, Are Induced in  
881 Arabidopsis during Infection with the Fungal Biotroph Erysiphe Cichoracearum.” *Plant  
882 Physiology* 132 (2): 821–29.

883 Frye, C. A., and R. W. Innes. 1998. “An Arabidopsis Mutant with Enhanced Resistance to  
884 Powdery Mildew.” *The Plant Cell* 10 (6): 947–56.

885 Frye, Catherine A., Dingzhong Tang, and Roger W. Innes. 2001. “Negative Regulation of  
886 Defense Responses in Plants by a Conserved MAPKK Kinase.” *Proceedings of the National  
887 Academy of Sciences* 98 (1): 373–78.

888 Gao, Huiling, Yu Gao, Fei Zhang, Baoling Liu, Chunli Ji, Jinai Xue, Lixia Yuan, and Runzhi Li.  
889 2021. “Functional Characterization of an Novel Acyl-CoA:diacylglycerol Acyltransferase 3-  
890 3 (CsDGAT3-3) Gene from Camelina Sativa.” *Plant Science: An International Journal of  
891 Experimental Plant Biology* 303 (February): 110752.

892 Gaude, Nicole, Claire Bréhélin, Gilbert Tischendorf, Felix Kessler, and Peter Dörmann. 2007.  
893 “Nitrogen Deficiency in Arabidopsis Affects Galactolipid Composition and Gene  
894 Expression and Results in Accumulation of Fatty Acid Phytol Esters.” *The Plant Journal:  
895 For Cell and Molecular Biology* 49 (4): 729–39.

896 Ghosh, S., K. A. Hudak, E. B. Dumbroff, and J. E. Thompson. 1994. “Release of Photosynthetic  
897 Protein Catabolites by Blebbing from Thylakoids.” *Plant Physiology* 106 (4): 1547–53.

898 Glawe, Dean A. 2008. “The Powdery Mildews: A Review of the World’s Most Familiar (yet  
899 Poorly Known) Plant Pathogens.” *Annual Review of Phytopathology* 46: 27–51.

900 Guzha, Athanas, Payton Whitehead, Till Ischebeck, and Kent D. Chapman. 2023. “Lipid  
901 Droplets: Packing Hydrophobic Molecules Within the Aqueous Cytoplasm.” *Annual Review  
902 of Plant Biology* 74 (1): 195–223.

903 Han, Longyan, Yuhui Zhai, Yumeng Wang, Xiangrui Shi, Yanfeng Xu, Shuguang Gao, Man  
904 Zhang, Jianrang Luo, and Qingyu Zhang. 2022. “Diacylglycerol Acyltransferase 3(DGAT3)  
905 Is Responsible for the Biosynthesis of Unsaturated Fatty Acids in Vegetative Organs of  
906 *Paeonia Rockii*.” *International Journal of Molecular Sciences* 23 (22).  
907 <https://doi.org/10.3390/ijms232214390>.

908 Hernández, M. Luisa, and Francisco Javier Cejudo. 2021. “Chloroplast Lipids Metabolism and  
909 Function. A Redox Perspective.” *Frontiers in Plant Science* 12 (August): 712022.

910 Hernández, M. Luisa, Lynne Whitehead, Zhesi He, Valeria Gazda, Alison Gilday, Ekaterina  
911 Kozhevnikova, Fabián E. Vaistij, Tony R. Larson, and Ian A. Graham. 2012. “A Cytosolic  
912 Acyltransferase Contributes to Triacylglycerol Synthesis in Sucrose-Rescued *Arabidopsis*  
913 Seed Oil Catabolism Mutants.” *Plant Physiology* 160 (1): 215–25.

914 Hözl, Georg, and Peter Dörmann. 2019. “Chloroplast Lipids and Their Biosynthesis.” *Annual  
915 Review of Plant Biology* 70 (April): 51–81.

916 Hunziker, Pascal, Hassan Ghareeb, Lena Wagenknecht, Christoph Crocoll, Barbara Ann Halkier,  
917 Volker Lipka, and Alexander Schulz. 2020. “De Novo Indol-3-Ylmethyl Glucosinolate  
918 Biosynthesis, and Not Long-Distance Transport, Contributes to Defence of *Arabidopsis*  
919 against Powdery Mildew.” *Plant, Cell & Environment* 43 (6): 1571–83.

920 Jessen, Dirk, Charlotte Roth, Marcel Wiermer, and Martin Fulda. 2015. “Two Activities of  
921 Long-Chain Acyl-Coenzyme A Synthetase Are Involved in Lipid Trafficking between the  
922 Endoplasmic Reticulum and the Plastid in *Arabidopsis*.” *Plant Physiology* 167 (2): 351–66.

923 Jiang, Yina, Wanxiao Wang, Qiu Jin Xie, Na Liu, Lixia Liu, Dapeng Wang, Xiaowei Zhang, et al.  
924 2017. “Plants Transfer Lipids to Sustain Colonization by Mutualistic Mycorrhizal and  
925 Parasitic Fungi.” *Science* 356 (6343): 1172–75.

926 Kachroo, Aardra, and Pradeep Kachroo. 2009. “Fatty Acid-Derived Signals in Plant Defense.”  
927 *Annual Review of Phytopathology* 47 (1): 153–76.

928 Kameoka, Hiromu, and Caroline Gutjahr. 2022. “Functions of Lipids in Development and  
929 Reproduction of Arbuscular Mycorrhizal Fungi.” *Plant & Cell Physiology* 63 (10): 1356–  
930 65.

931 Kameoka, Hiromu, Taro Maeda, Nao Okuma, and Masayoshi Kawaguchi. 2019. “Structure-  
932 Specific Regulation of Nutrient Transport and Metabolism in Arbuscular Mycorrhizal  
933 Fungi.” *Plant & Cell Physiology* 60 (10): 2272–81.

934 Katavic, V., D. W. Reed, D. C. Taylor, E. M. Giblin, D. L. Barton, J. Zou, S. L. Mackenzie, P. S.  
935 Covello, and L. Kunst. 1995. “Alteration of Seed Fatty Acid Composition by an Ethyl  
936 Methanesulfonate-Induced Mutation in *Arabidopsis Thaliana* Affecting Diacylglycerol  
937 Acyltransferase Activity.” *Plant Physiology* 108 (1): 399–409.

938 Kaup, Marianne T., Carol D. Froese, and John E. Thompson. 2002. “A Role for Diacylglycerol  
939 Acyltransferase during Leaf Senescence.” *Plant Physiology* 129 (4): 1616–26.

940 Kim, Sangwoo, Yasuyo Yamaoka, Hirofumi Ono, Hanul Kim, Donghwan Shim, Masayoshi  
941 Maeshima, Enrico Martinoia, Edgar B. Cahoon, Ikuo Nishida, and Youngsook Lee. 2013.  
942 “AtABCA9 Transporter Supplies Fatty Acids for Lipid Synthesis to the Endoplasmic  
943 Reticulum.” *Proceedings of the National Academy of Sciences of the United States of  
944 America* 110 (2): 773–78.

945 Klepikova, Anna V., Artem S. Kasianov, Evgeny S. Gerasimov, Maria D. Logacheva, and

946 Aleksey A. Penin. 2016. “A High Resolution Map of the *Arabidopsis* Thaliana  
947 Developmental Transcriptome Based on RNA-Seq Profiling.” *The Plant Journal: For Cell*  
948 *and Molecular Biology* 88 (6): 1058–70.

949 Koh, Serry, Aurélie André, Herb Edwards, David Ehrhardt, and Shauna Somerville. 2005.  
950 “*Arabidopsis* Thaliana Subcellular Responses to Compatible Erysiphe Cichoracearum  
951 Infections.” *The Plant Journal: For Cell and Molecular Biology* 44 (3): 516–29.

952 Kumar, Aruna, Aarti Sharma, and Kailash C. Upadhyaya. 2016. “Vegetable Oil: Nutritional and  
953 Industrial Perspective.” *Current Genomics* 17 (3): 230–40.

954 Liang, Peng, Songyu Liu, Feng Xu, Shuqin Jiang, Jun Yan, Qiguang He, Wenbo Liu, et al. 2018.  
955 “Powdery Mildews Are Characterized by Contracted Carbohydrate Metabolism and Diverse  
956 Effectors to Adapt to Obligate Biotrophic Lifestyle.” *Frontiers in Microbiology* 9  
957 (December): 3160.

958 Lippold, Felix, Katharina vom Dorp, Marion Abraham, Georg Hözl, Vera Wewer, Jenny  
959 Lindberg Yilmaz, Ida Lager, et al. 2012. “Fatty Acid Phytyl Ester Synthesis in Chloroplasts  
960 of *Arabidopsis*.” *The Plant Cell* 24 (5): 2001–14.

961 Liu, Simu, Lisa M. Bartnikas, Sigrid M. Volko, Frederick M. Ausubel, and Dingzhong Tang.  
962 2016. “Mutation of the Glucosinolate Biosynthesis Enzyme Cytochrome P450 83A1  
963 Monooxygenase Increases Camalexin Accumulation and Powdery Mildew Resistance.”  
964 *Frontiers in Plant Science* 7 (March): 227.

965 Luginbuehl, Leonie H., Guillaume N. Menard, Smita Kurup, Harrie Van Erp, Guru V.  
966 Radhakrishnan, Andrew Breakspear, Giles E. D. Oldroyd, and Peter J. Eastmond. 2017.  
967 “Fatty Acids in Arbuscular Mycorrhizal Fungi Are Synthesized by the Host Plant.” *Science*  
968 356 (6343): 1175–78.

969 Lu, Junhao, Yang Xu, Juli Wang, Stacy D. Singer, and Guanqun Chen. 2020. “The Role of  
970 Triacylglycerol in Plant Stress Response.” *Plants* 9 (4).  
971 <https://doi.org/10.3390/plants9040472>.

972 Lundquist, Peter K., Anton Poliakov, Nazmul H. Bhuiyan, Boris Zyballov, Qi Sun, and Klaas J.  
973 van Wijk. 2012. “The Functional Network of the *Arabidopsis* Plastoglobule Proteome Based  
974 on Quantitative Proteomics and Genome-Wide Coexpression Analysis.” *Plant Physiology*  
975 158 (3): 1172–92.

976 Lü, Shiyu, Tao Song, Dylan K. Kosma, Eugene P. Parsons, Owen Rowland, and Matthew A.  
977 Jenks. 2009. “*Arabidopsis* CER8 Encodes LONG-CHAIN ACYL-COA SYNTHETASE 1  
978 (LACS1) That Has Overlapping Functions with LACS2 in Plant Wax and Cutin Synthesis.”  
979 *The Plant Journal: For Cell and Molecular Biology* 59 (4): 553–64.

980 MacLean, Allyson M., Armando Bravo, and Maria J. Harrison. 2017. “Plant Signaling and  
981 Metabolic Pathways Enabling Arbuscular Mycorrhizal Symbiosis.” *The Plant Cell* 29 (10):  
982 2319–35.

983 Mats X. Andersson, J. Magnus Kjellberg, and Anna Stina Sandelius. 2001. “Chloroplast  
984 Biogenesis. Regulation of Lipid Transport to the Thylakoid in Chloroplasts Isolated from  
985 Expanding and Fully Expanded Leaves of Pea.” *Plant Physiology* 127 (1): 184–93.

986 McRae, Amanda G., Jyoti Taneja, Kathleen Yee, Xinyi Shi, Sajeet Haridas, Kurt LaButti,  
987 Vasanth Singan, Igor V. Grigoriev, and Mary C. Wildermuth. 2023. “Spray-Induced Gene  
988 Silencing to Identify Powdery Mildew Gene Targets and Processes for Powdery Mildew  
989 Control.” *Molecular Plant Pathology* 24 (9): 1168–83.

990 Micali, Cristina, Katharina Göllner, Matt Humphry, Chiara Consonni, and Ralph Panstruga.  
991 2008. “The Powdery Mildew Disease of *Arabidopsis*: A Paradigm for the Interaction

992        between Plants and Biotrophic Fungi.” *The Arabidopsis Book / American Society of Plant*  
993        *Biologists* 6 (October): e0115.

994        Michel, Elena J. S., Lalit Ponnala, and Klaas J. van Wijk. 2021. “Tissue-Type Specific  
995        Accumulation of the Plastoglobular Proteome, Transcriptional Networks, and Plastoglobular  
996        Functions.” *Journal of Experimental Botany* 72 (13): 4663–79.

997        Moellering, Eric R., Bagyalakshmi Muthan, and Christoph Benning. 2010. “Freezing Tolerance  
998        in Plants Requires Lipid Remodeling at the Outer Chloroplast Membrane.” *Science* 330  
999        (6001): 226–28.

1000       Murphy, Robert C. 2014. *Tandem Mass Spectrometry of Lipids: Molecular Analysis of Complex*  
1001       *Lipids*. Royal Society of Chemistry.

1002       Okazaki, Yozo, and Kazuki Saito. 2014. “Roles of Lipids as Signaling Molecules and Mitigators  
1003       during Stress Response in Plants.” *The Plant Journal: For Cell and Molecular Biology* 79  
1004       (4): 584–96.

1005       Pfleger, Brian F., Michael Gossing, and Jens Nielsen. 2015. “Metabolic Engineering Strategies  
1006       for Microbial Synthesis of Oleochemicals.” *Metabolic Engineering* 29 (May): 1–11.

1007       Przybyla-Toscano, Jonathan, Mélanie Roland, Frédéric Gaymard, Jérémie Couturier, and Nicolas  
1008       Rouhier. 2018. “Roles and Maturation of Iron-Sulfur Proteins in Plastids.” *Journal of*  
1009       *Biological Inorganic Chemistry: JBIC: A Publication of the Society of Biological Inorganic*  
1010       *Chemistry* 23 (4): 545–66.

1011       Regmi, Anushobha, Jay Shockey, Hari Kiran Kotapati, and Philip D. Bates. 2020. “Oil-  
1012       Producing Metabolons Containing DGAT1 Use Separate Substrate Pools from Those  
1013       Containing DGAT2 or PDAT.” *Plant Physiology* 184 (2): 720–37.

1014       Reuber, T. L., J. M. Plotnikova, J. Dewdney, E. E. Rogers, W. Wood, and F. M. Ausubel. 1998.  
1015       “Correlation of Defense Gene Induction Defects with Powdery Mildew Susceptibility in  
1016       Arabidopsis Enhanced Disease Susceptibility Mutants.” *The Plant Journal: For Cell and*  
1017       *Molecular Biology* 16 (4): 473–85.

1018       Saha, Saikat, Balaji Enugutti, Sona Rajakumari, and Ram Rajasekharan. 2006. “Cytosolic  
1019       Triacylglycerol Biosynthetic Pathway in Oilseeds. Molecular Cloning and Expression of  
1020       Peanut Cytosolic Diacylglycerol Acyltransferase.” *Plant Physiology* 141 (4): 1533–43.

1021       Shimada, Takashi L., Makoto Hayashi, and Ikuko Hara-Nishimura. 2017. “Membrane Dynamics  
1022       and Multiple Functions of Oil Bodies in Seeds and Leaves.” *Plant Physiology* 176 (1): 199–  
1023       207.

1024       Shimada, Takashi L., Yoshitaka Takano, Tomoo Shimada, Masayuki Fujiwara, Yoichiro Fukao,  
1025       Masashi Mori, Yozo Okazaki, et al. 2014. “Leaf Oil Body Functions as a Subcellular  
1026       Factory for the Production of a Phytoalexin in Arabidopsis.” *Plant Physiology* 164 (1): 105–  
1027       18.

1028       Shiva, Sunitha, Thilani Samarakoon, Kaleb A. Lowe, Charles Roach, Hieu Sy Vu, Madeline  
1029       Colter, Hollie Porras, et al. 2020. “Leaf Lipid Alterations in Response to Heat Stress of  
1030       Arabidopsis Thaliana.” *Plants* 9 (7). <https://doi.org/10.3390/plants9070845>.

1031       Shiva, Sunitha, Hieu Sy Vu, Mary R. Roth, Zhenguo Zhou, Shantan Reddy Marepally, Daya  
1032       Sagar Nune, Gerald H. Lushington, Mahesh Visvanathan, and Ruth Welti. 2013. “Lipidomic  
1033       Analysis of Plant Membrane Lipids by Direct Infusion Tandem Mass Spectrometry.”  
1034       *Methods in Molecular Biology* 1009: 79–91.

1035       Smith, Matthew D., Donny D. Licatalosi, and John E. Thompson. 2000. “Co-Association of  
1036       Cytochrome F Catabolites and Plastid-Lipid-Associated Protein with Chloroplast Lipid  
1037       Particles1.” *Plant Physiology* 124 (1): 211–22.

1038 Spanu, Pietro D. 2012. "The Genomics of Obligate (and Nonobligate) Biotrophs." *Annual  
1039 Review of Phytopathology* 50 (May): 91–109.

1040 Springer, Armin, Chulhee Kang, Sachin Rustgi, Diter von Wettstein, Christiane Reinbothe,  
1041 Stephan Pollmann, and Steffen Reinbothe. 2016. "Programmed Chloroplast Destruction  
1042 during Leaf Senescence Involves 13-Lipoxygenase (13-LOX)." *Proceedings of the National  
1043 Academy of Sciences* 113 (12): 3383–88.

1044 Sutton, P. N., M. J. Henry, and J. L. Hall. 1999. "Glucose, and Not Sucrose, Is Transported from  
1045 Wheat to Wheat Powdery Mildew." *Planta* 208 (3): 426–30.

1046 Swarbrick, Philip J., Paul Schulze-Lefert, and Julie D. Scholes. 2006. "Metabolic Consequences  
1047 of Susceptibility and Resistance (race-Specific and Broad-Spectrum) in Barley Leaves  
1048 Challenged with Powdery Mildew." *Plant, Cell & Environment* 29 (6): 1061–76.

1049 Tang, Dingzhong, Michael T. Simonich, and Roger W. Innes. 2007. "Mutations in LACS2, a  
1050 Long-Chain Acyl-Coenzyme A Synthetase, Enhance Susceptibility to Avirulent  
1051 Pseudomonas Syringae but Confer Resistance to Botrytis Cinerea in Arabidopsis." *Plant  
1052 Physiology* 144 (2): 1093–1103.

1053 Tournayre, Jeremy, Matthieu Reichstadt, Laurent Parry, Pierre Fafournoux, and Celine Jousse.  
1054 2019. "'Do My qPCR Calculation', a Web Tool." *Bioinformation* 15 (5): 369–72.

1055 Tsitsigiannis, Dimitrios I., Terri M. Kowieski, Robert Zarnowski, and Nancy P. Keller. 2004.  
1056 "Endogenous Lipogenic Regulators of Spore Balance in Aspergillus Nidulans." *Eukaryotic  
1057 Cell* 3 (6): 1398–1411.

1058 Vallochi, Adriana Lima, Livia Teixeira, Karina da Silva Oliveira, Clarissa Menezes Maya-  
1059 Monteiro, and Patricia T. Bozza. 2018. "Lipid Droplet, a Key Player in Host-Parasite  
1060 Interactions." *Frontiers in Immunology* 9 (May): 1022.

1061 Vanhercke, Thomas, John M. Dyer, Robert T. Mullen, Aruna Kilaru, Md Mahbubur Rahman,  
1062 James R. Petrie, Allan G. Green, Olga Yurchenko, and Surinder P. Singh. 2019. "Metabolic  
1063 Engineering for Enhanced Oil in Biomass." *Progress in Lipid Research* 74 (April): 103–29.

1064 Vanhercke, Thomas, Anna El Tahchy, Pushkar Shrestha, Xue-Rong Zhou, Surinder P. Singh,  
1065 and James R. Petrie. 2013. "Synergistic Effect of WRI1 and DGAT1 Coexpression on  
1066 Triacylglycerol Biosynthesis in Plants." *FEBS Letters* 587 (4): 364–69.

1067 Vidi, Pierre-Alexandre, Marion Kanwischer, Sacha Baginsky, Jotham R. Austin, Gabor Csucs,  
1068 Peter Dörmann, Felix Kessler, and Claire Bréhélin. 2006. "Tocopherol Cyclase (VTE1)  
1069 Localization and Vitamin E Accumulation in Chloroplast Plastoglobule Lipoprotein  
1070 Particles." *The Journal of Biological Chemistry* 281 (16): 11225–34.

1071 Wang, Liping, Wenyun Shen, Michael Kazachkov, Guanqun Chen, Qilin Chen, Anders S.  
1072 Carlsson, Sten Stymne, Randall J. Weselake, and Jitao Zou. 2012. "Metabolic Interactions  
1073 between the Lands Cycle and the Kennedy Pathway of Glycerolipid Synthesis in  
1074 Arabidopsis Developing Seeds." *The Plant Cell* 24 (11): 4652–69.

1075 Wang, Wenming, Yingqiang Wen, Robert Berkey, and Shunyuan Xiao. 2009. "Specific  
1076 Targeting of the Arabidopsis Resistance Protein RPW8.2 to the Interfacial Membrane  
1077 Encasing the Fungal Haustorium Renders Broad-Spectrum Resistance to Powdery Mildew."  
1078 *The Plant Cell* 21 (9): 2898–2913.

1079 Welti, Ruth, Weiqi Li, Maoyin Li, Yongming Sang, Homigol Biesiada, Han-E Zhou, C. B.  
1080 Rajashekhar, Todd D. Williams, and Xuemin Wang. 2002. "Profiling Membrane Lipids in  
1081 Plant Stress Responses. Role of Phospholipase D Alpha in Freezing-Induced Lipid Changes  
1082 in Arabidopsis." *The Journal of Biological Chemistry* 277 (35): 31994–2.

1083 Weng, Hua, Isabel Molina, Jay Shockley, and John Browse. 2010. "Organ Fusion and Defective

1084 Cuticle Function in a lacs1 lacs2 Double Mutant of Arabidopsis.” *Planta* 231 (5): 1089–  
1085 1100.

1086 Weßling, Ralf, and Ralph Panstruga. 2012. “Rapid Quantification of Plant-Powdery Mildew  
1087 Interactions by qPCR and Conidiospore Counts.” *Plant Methods* 8 (1): 35.

1088 Wildermuth, Mary C. 2010. “Modulation of Host Nuclear Ploidy: A Common Plant Biotroph  
1089 Mechanism.” *Current Opinion in Plant Biology* 13 (4): 449–58.

1090 Wildermuth, Mary C., Michael A. Steinwand, Amanda G. McRae, Johan Jaenisch, and Divya  
1091 Chandran. 2017. “Adapted Biotroph Manipulation of Plant Cell Ploidy.” *Annual Review of  
1092 Phytopathology* 55 (August): 537–64.

1093 Winter, Debbie, Ben Vinegar, Hardeep Nahal, Ron Ammar, Greg V. Wilson, and Nicholas J.  
1094 Provart. 2007. “An ‘Electronic Fluorescent Pictograph’ Browser for Exploring and  
1095 Analyzing Large-Scale Biological Data Sets.” *PLoS One* 2 (8): e718.

1096 Xu, Changcheng, Jilian Fan, and John Shanklin. 2020. “Metabolic and Functional Connections  
1097 between Cytoplasmic and Chloroplast Triacylglycerol Storage.” *Progress in Lipid Research*  
1098 80 (November): 101069.

1099 Xu, Changcheng, and John Shanklin. 2016. “Triacylglycerol Metabolism, Function, and  
1100 Accumulation in Plant Vegetative Tissues.” *Annual Review of Plant Biology* 67 (April):  
1101 179–206.

1102 Xue, Jinai, Huiling Gao, Yinghong Xue, Ruixiang Shi, Mengmeng Liu, Lijun Han, Yu Gao, et  
1103 al. 2022. “Functional Characterization of Soybean Diacylglycerol Acyltransferase 3 in Yeast  
1104 and Soybean.” *Frontiers in Plant Science* 13 (May): 854103.

1105 Xu, Xiao-Yu, Hong-Kun Yang, Surinder P. Singh, Peter J. Sharp, and Qing Liu. 2018. “Genetic  
1106 Manipulation of Non-Classic Oilseed Plants for Enhancement of Their Potential as a  
1107 Biofactory for Triacylglycerol Production.” *Proceedings of the Estonian Academy of  
1108 Sciences: Engineering* 4 (4): 523–33.

1109 Yan, Bowei, Xiaoxuan Xu, Yingnan Gu, Ying Zhao, Xunchao Zhao, Lin He, Changjiang Zhao,  
1110 Zuotong Li, and Jingyu Xu. 2018. “Genome-Wide Characterization and Expression  
1111 Profiling of Diacylglycerol Acyltransferase Genes from Maize.” *Genome / National  
1112 Research Council Canada = Genome / Conseil National de Recherches Canada* 61 (10):  
1113 735–43.

1114 Yao, Hong-Yan, Yao-Qi Lu, Xiao-Li Yang, Xiao-Qing Wang, Zhipu Luo, De-Li Lin, Jia-Wei  
1115 Wu, and Hong-Wei Xue. 2023. “Arabidopsis Sec14 Proteins (SFH5 and SFH7) Mediate  
1116 Interorganelle Transport of Phosphatidic Acid and Regulate Chloroplast Development.”  
1117 *Proceedings of the National Academy of Sciences of the United States of America* 120 (6):  
1118 e2221637120.

1119 Yin, Xiangzhen, Xupeng Guo, Lizong Hu, Shuangshuang Li, Yuhong Chen, Jingqiao Wang,  
1120 Richard R-C Wang, Chengming Fan, and Zanmin Hu. 2022. “Genome-Wide  
1121 Characterization of DGATs and Their Expression Diversity Analysis in Response to Abiotic  
1122 Stresses in *Brassica Napus*.” *Plants* 11 (9). <https://doi.org/10.3390/plants11091156>.

1123 Ytterberg, A. Jimmy, Jean-Benoit Peltier, and Klaas J. van Wijk. 2006. “Protein Profiling of  
1124 Plastoglobules in Chloroplasts and Chromoplasts. A Surprising Site for Differential  
1125 Accumulation of Metabolic Enzymes.” *Plant Physiology* 140 (3): 984–97.

1126 Zhang, Meng, Jilian Fan, David C. Taylor, and John B. Ohlrogge. 2009. “DGAT1 and PDAT1  
1127 Acyltransferases Have Overlapping Functions in Arabidopsis Triacylglycerol Biosynthesis  
1128 and Are Essential for Normal Pollen and Seed Development.” *The Plant Cell* 21 (12): 3885–  
1129 3901.

1130 Zhao, Lifang, Vesna Katainic, Fengling Li, George W. Haughn, and Ljerka Kunst. 2010.  
1131 “Insertional Mutant Analysis Reveals That Long-Chain Acyl-CoA Synthetase 1 (LACS1),  
1132 but Not LACS8, Functionally Overlaps with LACS9 in Arabidopsis Seed Oil Biosynthesis.”  
1133 *The Plant Journal: For Cell and Molecular Biology* 64 (6): 1048–58.  
1134 Zhou, Xue-Rong, Sajina Bhandari, Brandon S. Johnson, Hari Kiran Kotapati, Doug K. Allen,  
1135 Thomas Vanhercke, and Philip D. Bates. 2019. “Reorganization of Acyl Flux through the  
1136 Lipid Metabolic Network in Oil-Accumulating Tobacco Leaves1 [OPEN].” *Plant*  
1137 *Physiology* 182 (2): 739–55.  
1138 Zhou, Xue-Rong, Pushkar Shrestha, Fang Yin, James R. Petrie, and Surinder P. Singh. 2013.  
1139 “AtDGAT2 Is a Functional Acyl-CoA:diacylglycerol Acyltransferase and Displays  
1140 Different Acyl-CoA Substrate Preferences than AtDGAT1.” *FEBS Letters* 587 (15): 2371–  
1141 76.  
1142 Zou, J., Y. Wei, C. Jako, A. Kumar, G. Selvaraj, and D. C. Taylor. 1999. “The Arabidopsis  
1143 Thaliana TAG1 Mutant Has a Mutation in a Diacylglycerol Acyltransferase Gene.” *The*  
1144 *Plant Journal: For Cell and Molecular Biology* 19 (6): 645–53.  
1145 Shiva, S., Vu, H. S., Roth, M. R., Zhou, Z., Marepally, S. R., Nune, D. S., Lushington, G. H.,  
1146 Visvanathan, M., & Welti, R. 2013). “Lipidomic analysis of plant membrane lipids by direct  
1147 infusion tandem mass spectrometry.” *Methods in molecular biology (Clifton, N.J.)*, 1009,  
1148 79–91. [https://doi.org/10.1007/978-1-62703-401-2\\_9](https://doi.org/10.1007/978-1-62703-401-2_9)  
1149

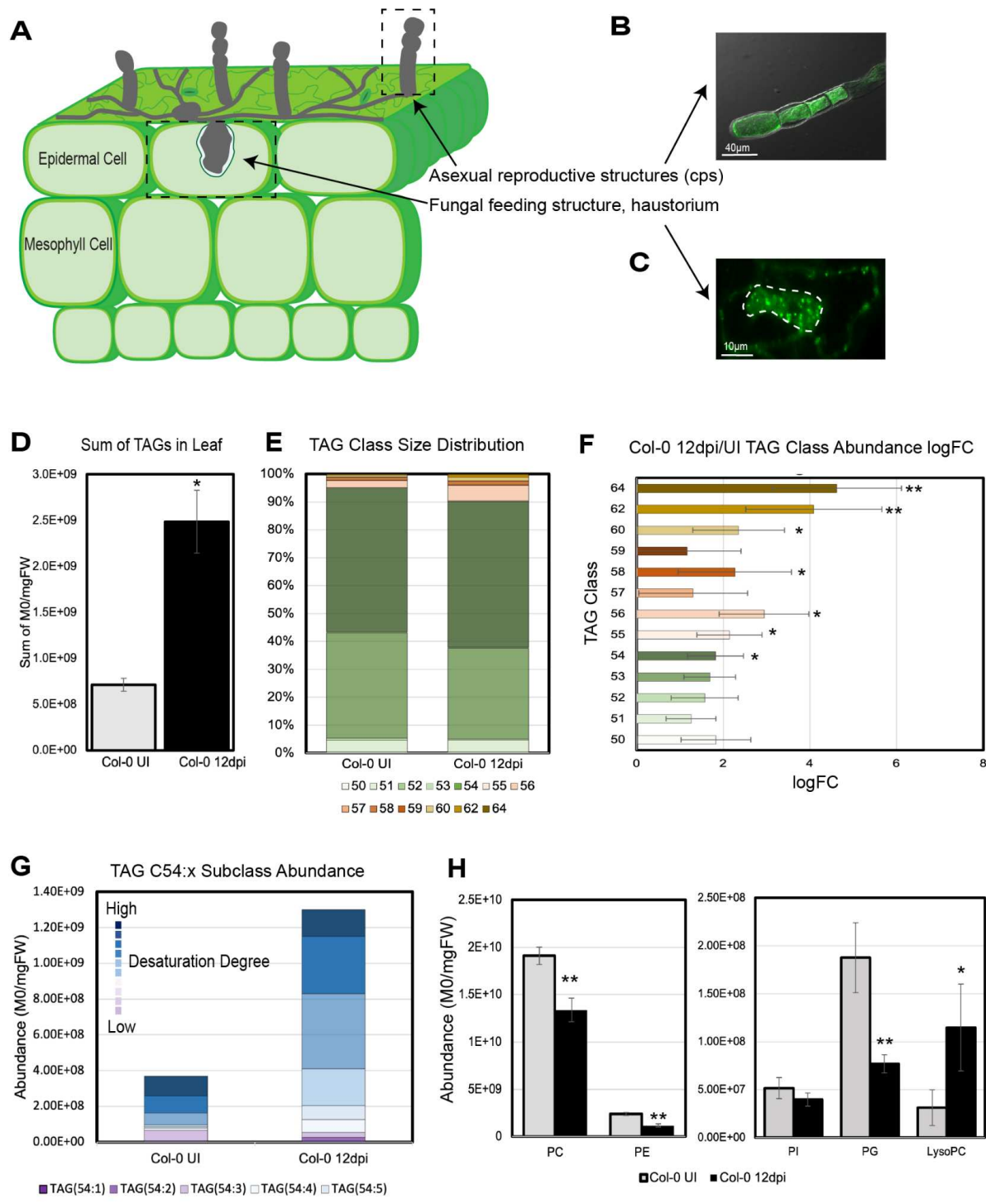
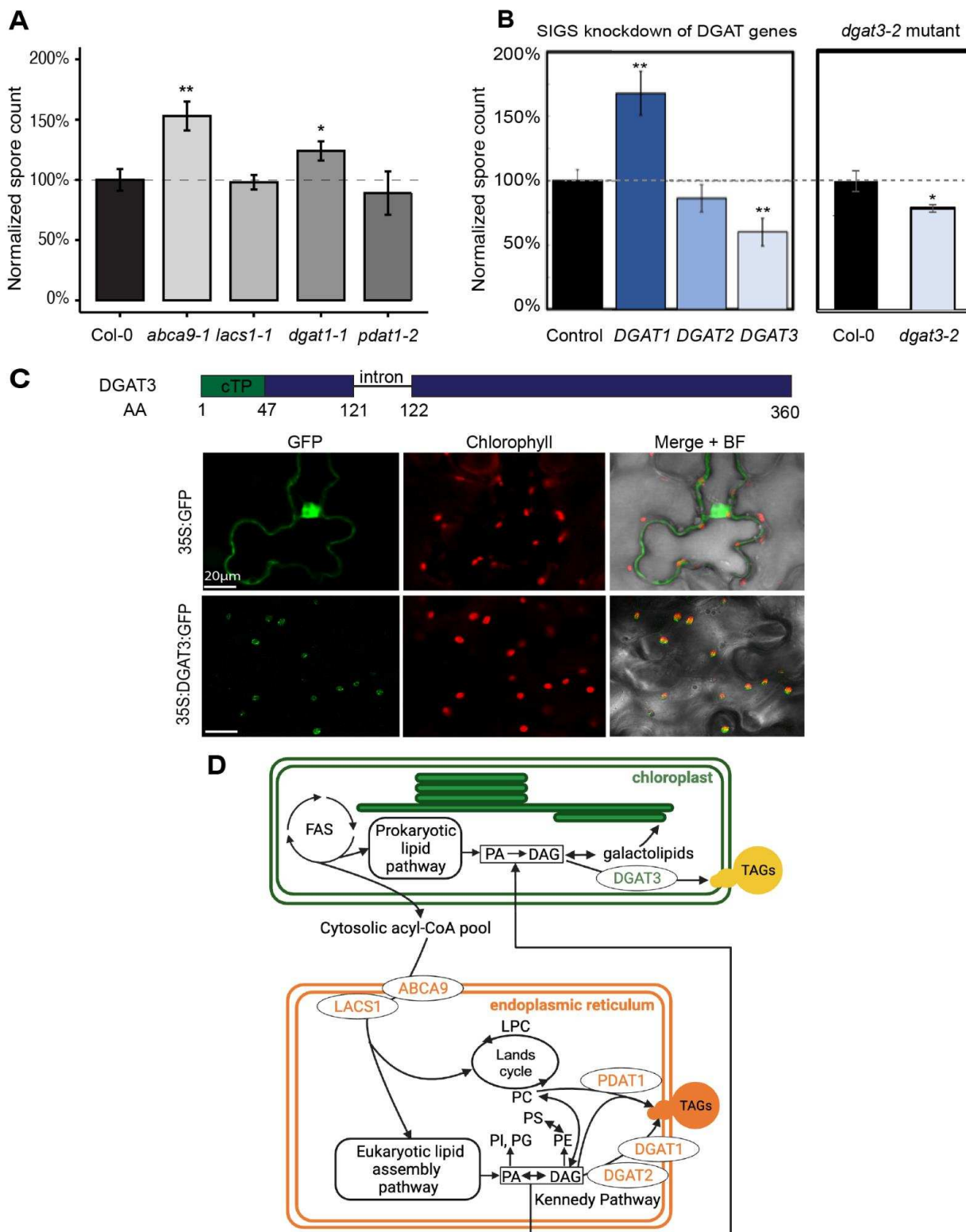


**Figure 1. TAG abundance is increased in infected Col-0 leaves.**

A) Cross-section depicting powdery mildew infection of *Arabidopsis* leaf at 5dpi. B-C) BODIPY 505/515 neutral lipid-stained powdery mildew structures: B) Asexual reproductive structure, conidiophore (cp), bar= 40μm. C) haustorium, bar= 10μm, white dashed line outlines haustorium. D) Total TAGs (C50-C64) detected in uninfected (UI) and 12dpi leaf lipid extracts ±STD, n= 3. E) Distribution of TAG classes in UI and 12dpi leaf lipid extracts. F) Log<sub>2</sub> fold change (LogFC) of TAG abundance by class in 12 dpi vs UI leaf lipid extracts ±STD, n= 3. G) Abundance of C54:x subclasses in UI and 12 dpi leaf lipid extracts. Assumes TAGs within this m/z range have similar desorption/ionization properties. H) Summed abundance of detected phospholipids (M0/mgFW) in UI (grey) and 12dpi (black) leaf lipid extracts ±STD, n= 3. Significance between UI and 12 dpi tested by 2-tailed T-test \* p ≤ 0.05, \*\* p ≤ 0.01.

1150  
1151  
1152  
1153  
1154  
1155  
1156  
1157  
1158  
1159

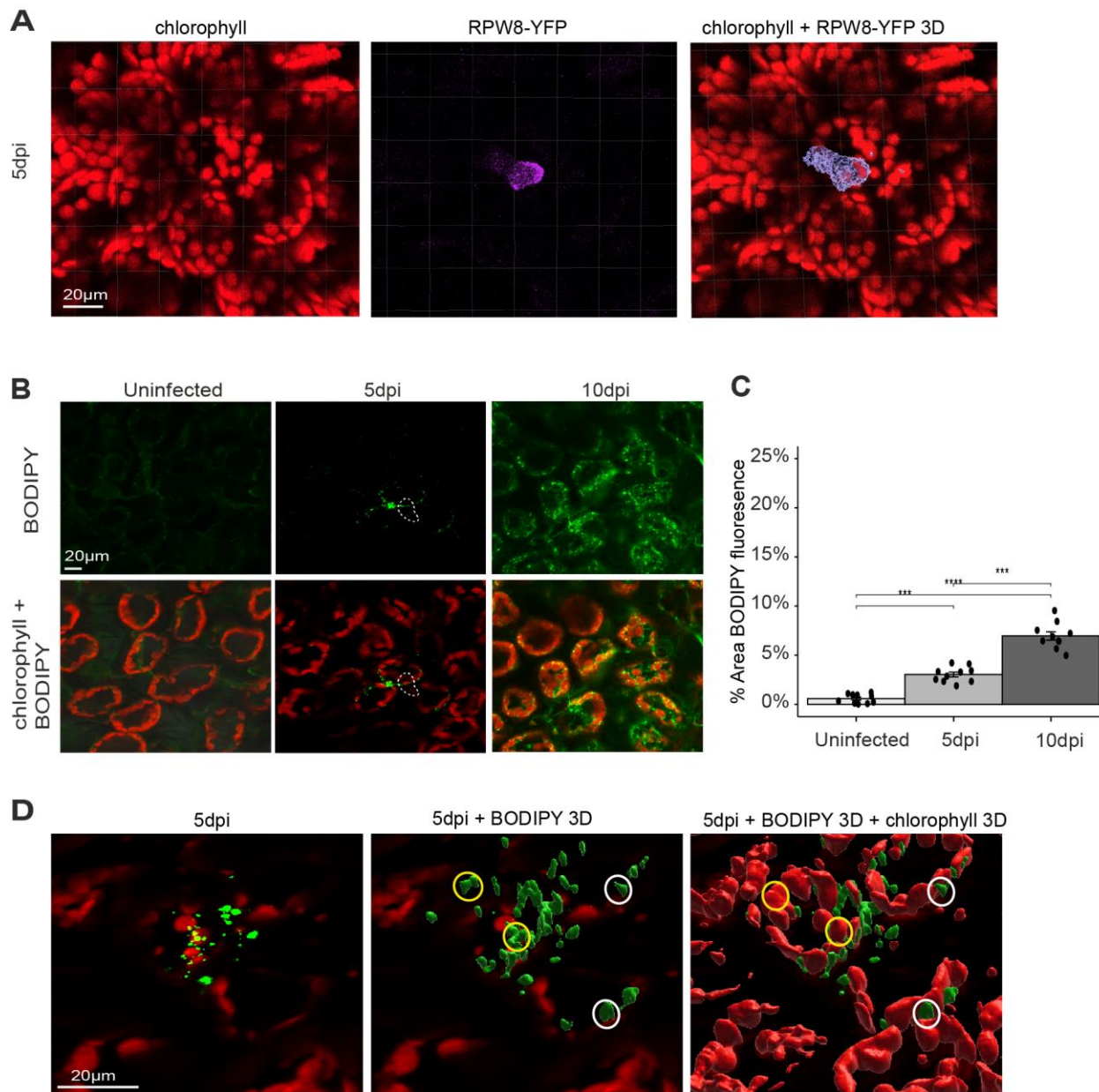


1160  
1161  
1162  
1163  
1164  
1165

**Figure 2. Canonical TAG synthesis in the ER hinders powdery mildew asexual reproduction while chloroplast-localized DGAT3 promotes it.**

A) Spore counts/mg leaf FW at 9dpi of mutants normalized to WT Col-0 for mutants involved in the canonical route for TAG synthesis in the ER ( $\pm$ STD, n= 5-8). B) Comparison of spore counts/mg leaf FW on WT plants with DGAT genes silenced via spray-induced gene silencing (SIGS) and *dgat3-2* mutant vs. WT at 9dpi ( $\pm$ STD, n= 4-8).

1166 Significance by 2-tailed T-Test \* $p \leq 0.05$ , \*\* $p \leq 0.01$ . C) AtDGAT3 protein is predicted to have a chloroplast transit  
1167 peptide by the DeepLoc 2.0 and LOCALIZER program. Confocal microscopy images of transient expression of  
1168 35S:AtDGAT3-GFP in *Nicotiana benthamiana*. D) Simplified model of tested players that may have contributed to  
1169 Arabidopsis TAG production. Abbreviations: ABCA, ATP-binding cassette A; BF, bright field; DAG, diacylglycerol;  
1170 DGAT, Diacylglyceroltransferase; FAS, fatty acid synthase complex; LACS, long chain acyl-CoA synthetase; LPC,  
1171 lysophosphatidylcholine; phosphatidic acid; PC, phosphatidylcholine; PE, phosphatidylethanolamine; PI,  
1172 phosphatidylinositol; PS, phosphatidylserine; PDAT, phospholipid:diacylglycerol acyltransferase; TAGs,  
1173 triacylglycerols. See Figure 1 for data on phospholipids.  
1174  
1175  
1176  
1177  
1178  
1179  
1180  
1181  
1182



1183

1184 **Figure 3. The powdery mildew induces the formation of lipid droplets in the host.**  
1185 A) Representative images of extrahaustorial membrane (EHM) targeted RPW8-YFP showing haustoria in epidermal  
1186 cell above three mesophyll cells in rosette leaves at 5 days post inoculation (5dpi). B) Representative images of  
1187 BODIPY 505/515 staining of neutral lipids in mesophyll cell layers of rosette leaves at 5 and 10 dpi. White dash line:  
1188 position of haustorium in the epidermal cell. C) Percentage of BODIPY fluorescence per image area of 50,000  $\mu\text{m}^2$   
1189 quantified by Imaris software. Data are mean  $\pm$  SD of 10 images. Significance is determined by one-way ANOVA. \*\*\*  
1190  $p \leq 0.001$ ,  $n = 10$ . D) Representative images of 3D reconstruction of BODIPY fluorescence (green) and chlorophyll  
1191 fluorescence (red) using Imaris software. Yellow circle: BODIPY fluorescent bodies inside the chloroplast. White  
1192 circle: BODIPY fluorescence bodies right next to the chloroplast.  
1193

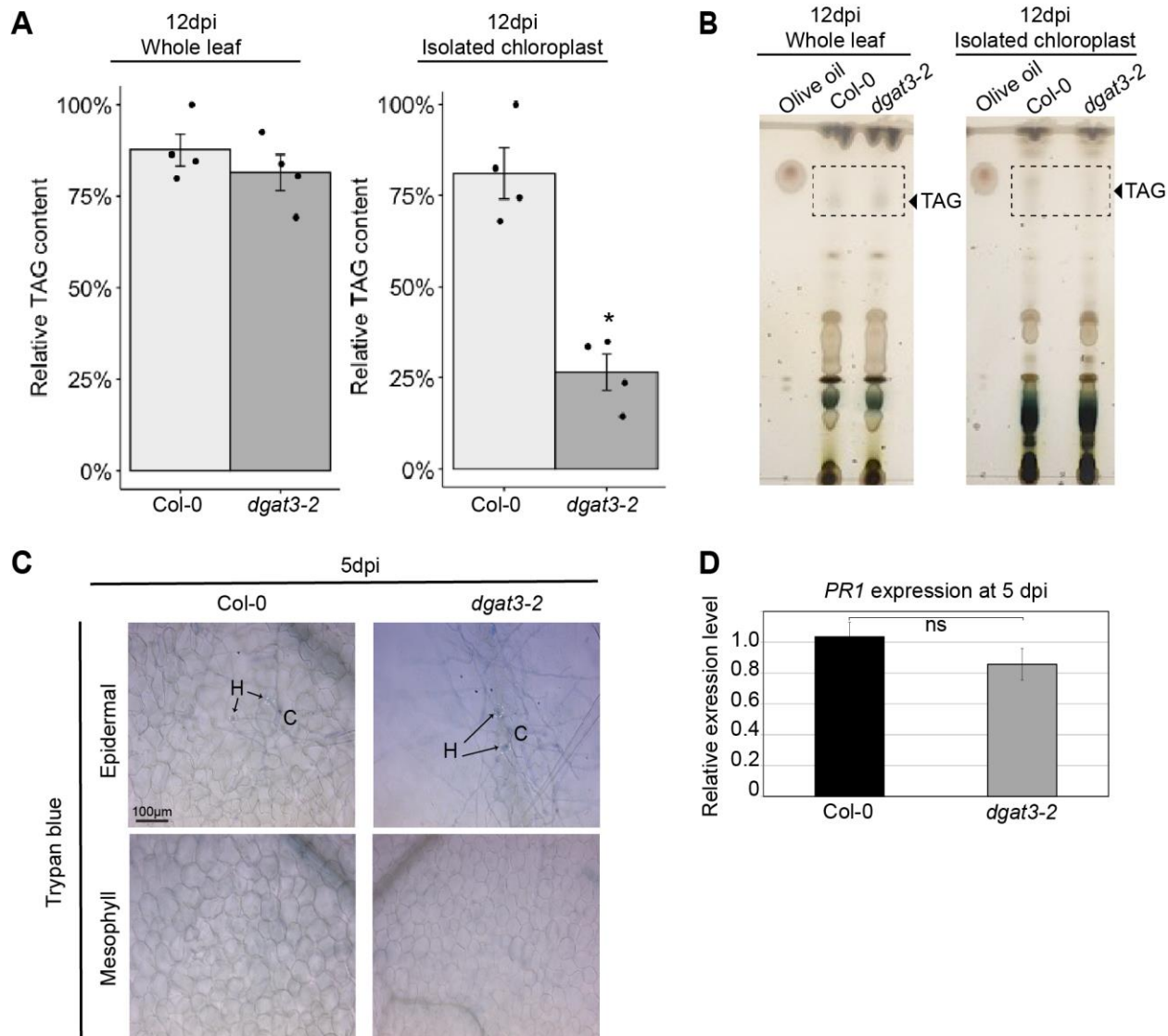


**Figure 4. TAG content in infected chloroplasts is decreased in dgat3-2 mutant while defense is not impacted.**

A) Relative TAG content in whole plants and chloroplasts of Col-0 and dgat3-2 at 12dpi were quantified by ImageJ software. Data are mean  $\pm$  SD of 4 biological replicates. Significance is determined by one-way ANOVA,  $*p \leq 0.05$ ,  $n = 4$ . B) Thin-layer chromatography of lipids extracted from either whole plant or isolated chloroplast at 12 dpi. Lipids were visualized with 5% sulfuric acid by charring. C) Trypan blue staining to visualize cell death in Col-0 and dgat3-2 plants at 5dpi. Top panel, epidermal cell layer. Bottom panel, underlying mesophyll cell layer. H, haustorium; C, germinated conidium. Note that fungal structures are stained slightly by trypan blue. D) Quantitative real-time PCR (qRT-PCR) analysis of PR1 expression in Col-0 and dgat3-2 plants at 5dpi normalized to housekeeping gene ACTIN-2 ( $\pm$  SD,  $n=3$ ); significance determined using unpaired, two-tailed Student's T-test. ns= not significantly different at  $p \leq 0.05$ .

1194  
1195

1196

1197

1198

1199

1200

1201

1202

1203

1204

1205

1206

1207

1208

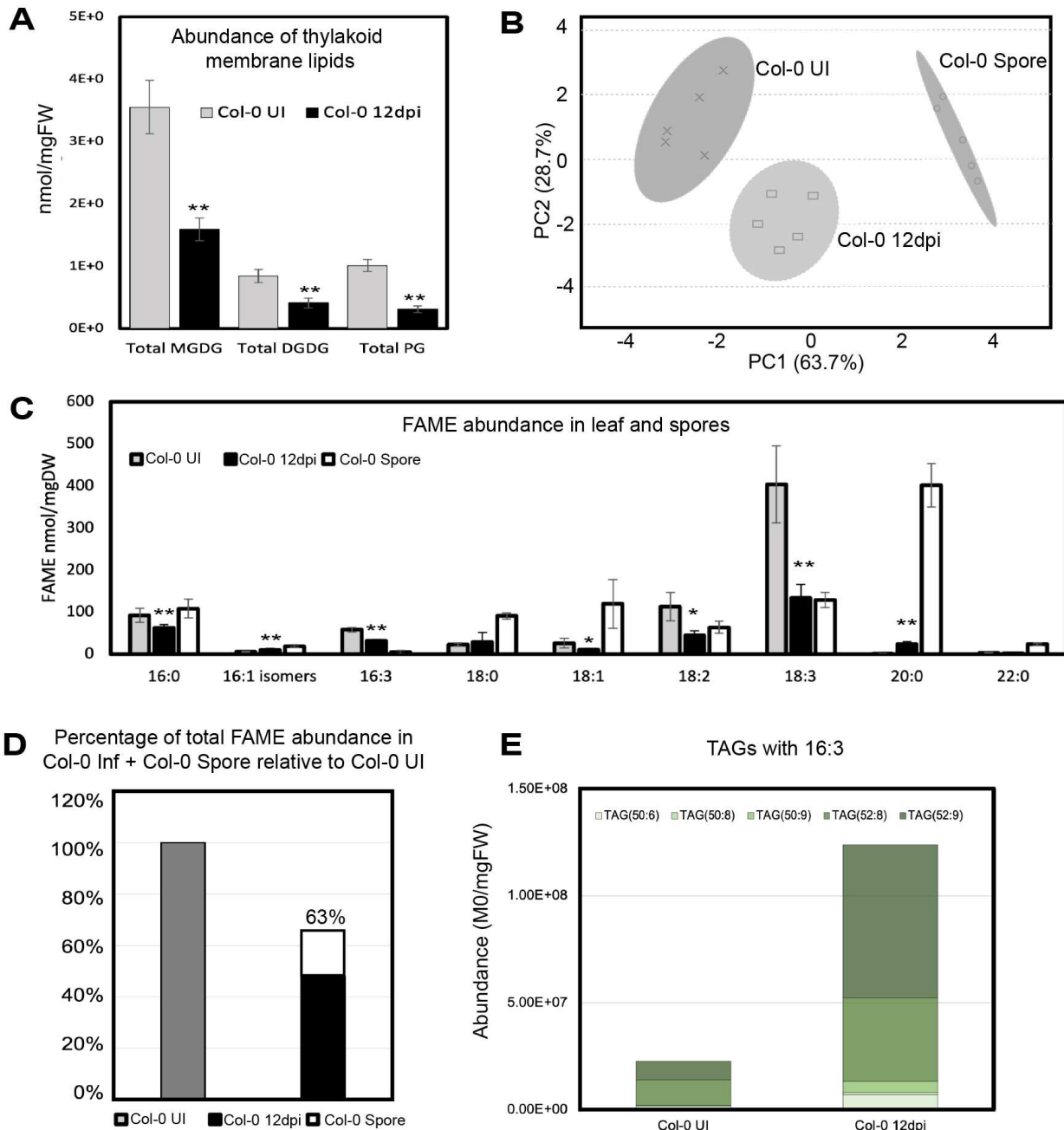
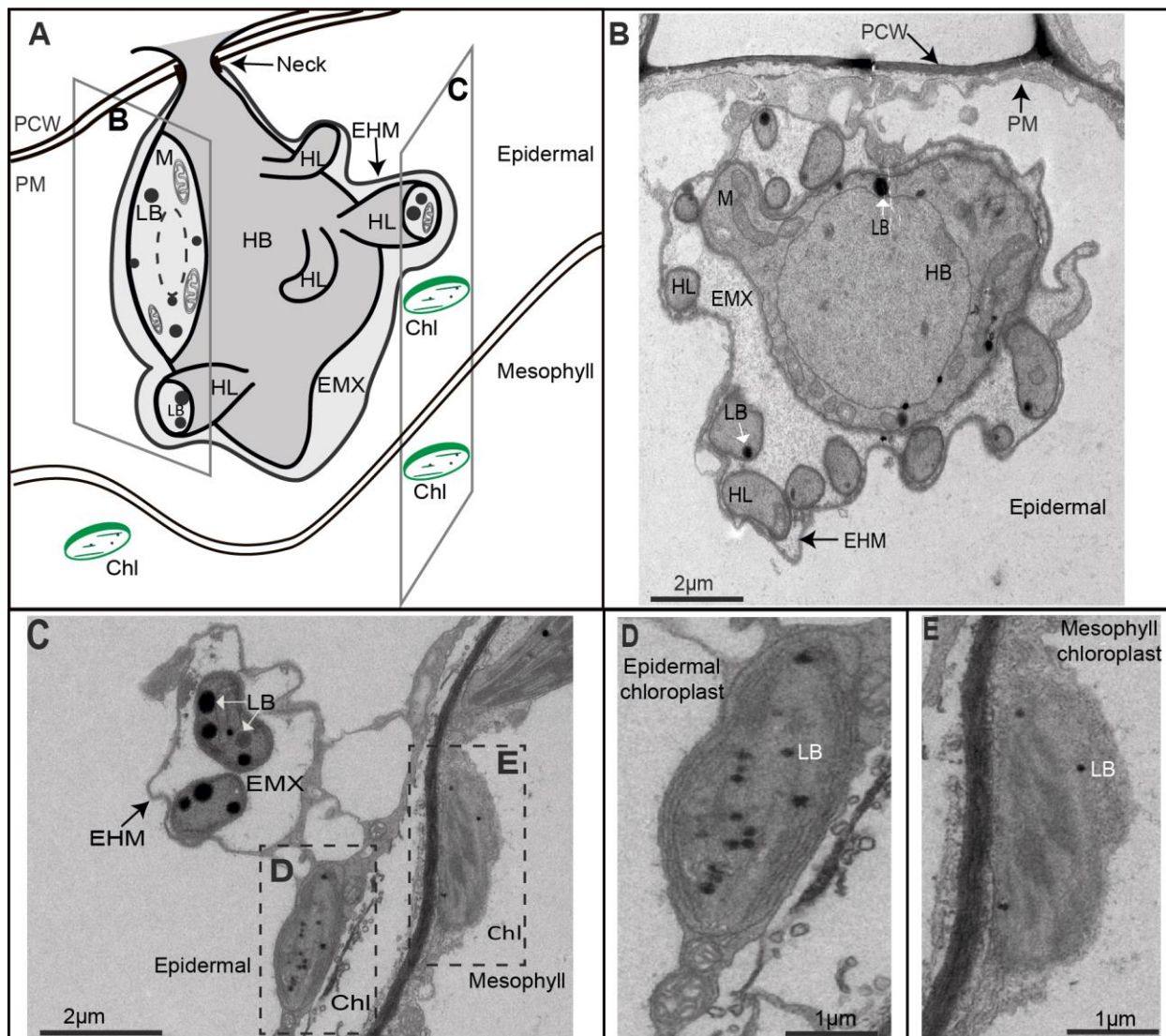


**Figure 5. Thylakoid membrane lipids and thylakoid-enriched FAs decrease with infection.**  
 1209  
 1210 A) Abundance of thylakoid membrane lipids (MGDG, monogalactosyldiacylglycerols; DGDG,  
 1211  
 1212  
 1213  
 1214  
 1215  
 1216  
 1217  
 1218  
 1219  
 1220  
 1221  
 1222  
 1223  
 1224  
 1225  
 1226  
 1227  
 1228  
 1229  
 1230  
 1231  
 1232  
 1233  
 1234  
 1235  
 1236  
 1237  
 1238  
 1239  
 1240  
 1241  
 1242  
 1243  
 1244  
 1245  
 1246  
 1247  
 1248  
 1249  
 1250  
 1251  
 1252  
 1253  
 1254  
 1255  
 1256  
 1257  
 1258  
 1259  
 1260  
 1261  
 1262  
 1263  
 1264  
 1265  
 1266  
 1267  
 1268  
 1269  
 1270  
 1271  
 1272  
 1273  
 1274  
 1275  
 1276  
 1277  
 1278  
 1279  
 1280  
 1281  
 1282  
 1283  
 1284  
 1285  
 1286  
 1287  
 1288  
 1289  
 1290  
 1291  
 1292  
 1293  
 1294  
 1295  
 1296  
 1297  
 1298  
 1299  
 1300  
 1301  
 1302  
 1303  
 1304  
 1305  
 1306  
 1307  
 1308  
 1309  
 1310  
 1311  
 1312  
 1313  
 1314  
 1315  
 1316  
 1317  
 1318  
 1319  
 1320  
 1321  
 1322  
 1323  
 1324  
 1325  
 1326  
 1327  
 1328  
 1329  
 1330  
 1331  
 1332  
 1333  
 1334  
 1335  
 1336  
 1337  
 1338  
 1339  
 1340  
 1341  
 1342  
 1343  
 1344  
 1345  
 1346  
 1347  
 1348  
 1349  
 1350  
 1351  
 1352  
 1353  
 1354  
 1355  
 1356  
 1357  
 1358  
 1359  
 1360  
 1361  
 1362  
 1363  
 1364  
 1365  
 1366  
 1367  
 1368  
 1369  
 1370  
 1371  
 1372  
 1373  
 1374  
 1375  
 1376  
 1377  
 1378  
 1379  
 1380  
 1381  
 1382  
 1383  
 1384  
 1385  
 1386  
 1387  
 1388  
 1389  
 1390  
 1391  
 1392  
 1393  
 1394  
 1395  
 1396  
 1397  
 1398  
 1399  
 1400  
 1401  
 1402  
 1403  
 1404  
 1405  
 1406  
 1407  
 1408  
 1409  
 1410  
 1411  
 1412  
 1413  
 1414  
 1415  
 1416  
 1417  
 1418  
 1419  
 1420  
 1421  
 1422  
 1423  
 1424  
 1425  
 1426  
 1427  
 1428  
 1429  
 1430  
 1431  
 1432  
 1433  
 1434  
 1435  
 1436  
 1437  
 1438  
 1439  
 1440  
 1441  
 1442  
 1443  
 1444  
 1445  
 1446  
 1447  
 1448  
 1449  
 1450  
 1451  
 1452  
 1453  
 1454  
 1455  
 1456  
 1457  
 1458  
 1459  
 1460  
 1461  
 1462  
 1463  
 1464  
 1465  
 1466  
 1467  
 1468  
 1469  
 1470  
 1471  
 1472  
 1473  
 1474  
 1475  
 1476  
 1477  
 1478  
 1479  
 1480  
 1481  
 1482  
 1483  
 1484  
 1485  
 1486  
 1487  
 1488  
 1489  
 1490  
 1491  
 1492  
 1493  
 1494  
 1495  
 1496  
 1497  
 1498  
 1499  
 1500  
 1501  
 1502  
 1503  
 1504  
 1505  
 1506  
 1507  
 1508  
 1509  
 1510  
 1511  
 1512  
 1513  
 1514  
 1515  
 1516  
 1517  
 1518  
 1519  
 1520  
 1521  
 1522  
 1523  
 1524  
 1525  
 1526  
 1527  
 1528  
 1529  
 1530  
 1531  
 1532  
 1533  
 1534  
 1535  
 1536  
 1537  
 1538  
 1539  
 1540  
 1541  
 1542  
 1543  
 1544  
 1545  
 1546  
 1547  
 1548  
 1549  
 1550  
 1551  
 1552  
 1553  
 1554  
 1555  
 1556  
 1557  
 1558  
 1559  
 1560  
 1561  
 1562  
 1563  
 1564  
 1565  
 1566  
 1567  
 1568  
 1569  
 1570  
 1571  
 1572  
 1573  
 1574  
 1575  
 1576  
 1577  
 1578  
 1579  
 1580  
 1581  
 1582  
 1583  
 1584  
 1585  
 1586  
 1587  
 1588  
 1589  
 1590  
 1591  
 1592  
 1593  
 1594  
 1595  
 1596  
 1597  
 1598  
 1599  
 1600  
 1601  
 1602  
 1603  
 1604  
 1605  
 1606  
 1607  
 1608  
 1609  
 1610  
 1611  
 1612  
 1613  
 1614  
 1615  
 1616  
 1617  
 1618  
 1619  
 1620  
 1621  
 1622  
 1623  
 1624  
 1625  
 1626  
 1627  
 1628  
 1629  
 1630  
 1631  
 1632  
 1633  
 1634  
 1635  
 1636  
 1637  
 1638  
 1639  
 1640  
 1641  
 1642  
 1643  
 1644  
 1645  
 1646  
 1647  
 1648  
 1649  
 1650  
 1651  
 1652  
 1653  
 1654  
 1655  
 1656  
 1657  
 1658  
 1659  
 1660  
 1661  
 1662  
 1663  
 1664  
 1665  
 1666  
 1667  
 1668  
 1669  
 1670  
 1671  
 1672  
 1673  
 1674  
 1675  
 1676  
 1677  
 1678  
 1679  
 1680  
 1681  
 1682  
 1683  
 1684  
 1685  
 1686  
 1687  
 1688  
 1689  
 1690  
 1691  
 1692  
 1693  
 1694  
 1695  
 1696  
 1697  
 1698  
 1699  
 1700  
 1701  
 1702  
 1703  
 1704  
 1705  
 1706  
 1707  
 1708  
 1709  
 1710  
 1711  
 1712  
 1713  
 1714  
 1715  
 1716  
 1717  
 1718  
 1719  
 1720  
 1721  
 1722  
 1723  
 1724  
 1725  
 1726  
 1727  
 1728  
 1729  
 1730  
 1731  
 1732  
 1733  
 1734  
 1735  
 1736  
 1737  
 1738  
 1739  
 1740  
 1741  
 1742  
 1743  
 1744  
 1745  
 1746  
 1747  
 1748  
 1749  
 1750  
 1751  
 1752  
 1753  
 1754  
 1755  
 1756  
 1757  
 1758  
 1759  
 1760  
 1761  
 1762  
 1763  
 1764  
 1765  
 1766  
 1767  
 1768  
 1769  
 1770  
 1771  
 1772  
 1773  
 1774  
 1775  
 1776  
 1777  
 1778  
 1779  
 1780  
 1781  
 1782  
 1783  
 1784  
 1785  
 1786  
 1787  
 1788  
 1789  
 1790  
 1791  
 1792  
 1793  
 1794  
 1795  
 1796  
 1797  
 1798  
 1799  
 1800  
 1801  
 1802  
 1803  
 1804  
 1805  
 1806  
 1807  
 1808  
 1809  
 1810  
 1811  
 1812  
 1813  
 1814  
 1815  
 1816  
 1817  
 1818  
 1819  
 1820  
 1821  
 1822  
 1823  
 1824  
 1825  
 1826  
 1827  
 1828  
 1829  
 1830  
 1831  
 1832  
 1833  
 1834  
 1835  
 1836  
 1837  
 1838  
 1839  
 1840  
 1841  
 1842  
 1843  
 1844  
 1845  
 1846  
 1847  
 1848  
 1849  
 1850  
 1851  
 1852  
 1853  
 1854  
 1855  
 1856  
 1857  
 1858  
 1859  
 1860  
 1861  
 1862  
 1863  
 1864  
 1865  
 1866  
 1867  
 1868  
 1869  
 1870  
 1871  
 1872  
 1873  
 1874  
 1875  
 1876  
 1877  
 1878  
 1879  
 1880  
 1881  
 1882  
 1883  
 1884  
 1885  
 1886  
 1887  
 1888  
 1889  
 1890  
 1891  
 1892  
 1893  
 1894  
 1895  
 1896  
 1897  
 1898  
 1899  
 1900  
 1901  
 1902  
 1903  
 1904  
 1905  
 1906  
 1907  
 1908  
 1909  
 1910  
 1911  
 1912  
 1913  
 1914  
 1915  
 1916  
 1917  
 1918  
 1919  
 1920  
 1921  
 1922  
 1923  
 1924  
 1925  
 1926  
 1927  
 1928  
 1929  
 1930  
 1931  
 1932  
 1933  
 1934  
 1935  
 1936  
 1937  
 1938  
 1939  
 1940  
 1941  
 1942  
 1943  
 1944  
 1945  
 1946  
 1947  
 1948  
 1949  
 1950  
 1951  
 1952  
 1953  
 1954  
 1955  
 1956  
 1957  
 1958  
 1959  
 1960  
 1961  
 1962  
 1963  
 1964  
 1965  
 1966  
 1967  
 1968  
 1969  
 1970  
 1971  
 1972  
 1973  
 1974  
 1975  
 1976  
 1977  
 1978  
 1979  
 1980  
 1981  
 1982  
 1983  
 1984  
 1985  
 1986  
 1987  
 1988  
 1989  
 1990  
 1991  
 1992  
 1993  
 1994  
 1995  
 1996  
 1997  
 1998  
 1999  
 2000  
 2001  
 2002  
 2003  
 2004  
 2005  
 2006  
 2007  
 2008  
 2009  
 2010  
 2011  
 2012  
 2013  
 2014  
 2015  
 2016  
 2017  
 2018  
 2019  
 2020  
 2021  
 2022  
 2023  
 2024  
 2025  
 2026  
 2027  
 2028  
 2029  
 2030  
 2031  
 2032  
 2033  
 2034  
 2035  
 2036  
 2037  
 2038  
 2039  
 2040  
 2041  
 2042  
 2043  
 2044  
 2045  
 2046  
 2047  
 2048  
 2049  
 2050  
 2051  
 2052  
 2053  
 2054  
 2055  
 2056  
 2057  
 2058  
 2059  
 2060  
 2061  
 2062  
 2063  
 2064  
 2065  
 2066  
 2067  
 2068  
 2069  
 2070  
 2071  
 2072  
 2073  
 2074  
 2075  
 2076  
 2077  
 2078  
 2079  
 2080  
 2081  
 2082  
 2083  
 2084  
 2085  
 2086  
 2087  
 2088  
 2089  
 2090  
 2091  
 2092  
 2093  
 2094  
 2095  
 2096  
 2097  
 2098  
 2099  
 20100  
 20101  
 20102  
 20103  
 20104  
 20105  
 20106  
 20107  
 20108  
 20109  
 20110  
 20111  
 20112  
 20113  
 20114  
 20115  
 20116  
 20117  
 20118  
 20119  
 20120  
 20121  
 20122  
 20123  
 20124  
 20125  
 20126  
 20127  
 20128  
 20129  
 20130  
 20131  
 20132  
 20133  
 20134  
 20135  
 20136  
 20137  
 20138  
 20139  
 20140  
 20141  
 20142  
 20143  
 20144  
 20145  
 20146  
 20147  
 20148  
 20149  
 20150  
 20151  
 20152  
 20153  
 20154  
 20155  
 20156  
 20157  
 20158  
 20159  
 20160  
 20161  
 20162  
 20163  
 20164  
 20165  
 20166  
 20167  
 20168  
 20169  
 20170  
 20171  
 20172  
 20173  
 20174  
 20175  
 20176  
 20177  
 20178  
 20179  
 20180  
 20181  
 20182  
 20183  
 20184  
 20185  
 20186  
 20187  
 20188  
 20189  
 20190  
 20191  
 20192  
 20193  
 20194  
 20195  
 20196  
 20197  
 20198  
 20199  
 20200  
 20201  
 20202  
 20203  
 20204  
 20205  
 20206  
 20207  
 20208  
 20209  
 20210  
 20211  
 20212  
 20213  
 20214  
 20215  
 20216  
 20217  
 20218  
 20219  
 20220  
 20221  
 20222  
 20223  
 20224  
 20225  
 20226  
 20227  
 20228  
 20229  
 20230  
 20231  
 20232  
 20233  
 20234  
 20235  
 20236  
 20237  
 20238  
 20239  
 20240  
 20241  
 20242  
 20243  
 20244  
 20245  
 20246  
 20247  
 20248  
 20249  
 20250  
 20251  
 20252  
 20253  
 20254  
 20255  
 20256  
 20257  
 20258  
 20259  
 20260  
 20261  
 20262  
 20263  
 20264  
 20265  
 20266  
 20267  
 20268  
 20269  
 20270  
 20271  
 20272  
 20273  
 20274  
 20275  
 20276  
 20277  
 20278  
 20279  
 20280  
 20281  
 20282  
 20283  
 20284  
 20285  
 20286  
 20287  
 20288  
 20289  
 20290  
 20291  
 20292  
 20293  
 20294  
 20295  
 20296  
 20297  
 20298  
 20299  
 20300  
 20301  
 20302  
 20303  
 20304  
 20305  
 20306  
 20307  
 20308  
 20309  
 20310  
 20311  
 20312  
 20313  
 20314  
 20315  
 20316  
 20317  
 20318  
 20319  
 20320  
 20321  
 20322  
 20323  
 20324  
 20325  
 20326  
 20327  
 20328  
 20329  
 20330  
 20331  
 20332  
 20333  
 20334  
 20335  
 20336  
 20337  
 20338  
 20339  
 20340  
 20341  
 20342  
 20343  
 20344  
 20345  
 20346  
 20347  
 20348  
 20349  
 20350  
 20351  
 20352  
 20353  
 20354  
 20355  
 20356  
 20357  
 20358  
 20359  
 20360  
 20361  
 20362  
 20363  
 20364  
 20365  
 20366  
 20367  
 20368  
 20369  
 20370  
 20371  
 20372  
 20373  
 20374  
 20375  
 20376  
 20377  
 20378  
 20379  
 20380  
 20381  
 20382  
 20383  
 20384  
 20385  
 20386  
 20387  
 20388  
 20389  
 20390  
 20391  
 20392  
 20393  
 20394  
 20395  
 20396  
 20397  
 20398  
 20399  
 20400  
 20401  
 20402  
 20403  
 20404  
 20405  
 20406  
 20407  
 20408



1218  
1219  
1220  
1221  
1222  
1223  
1224  
1225  
1226

**Figure 6. The powdery mildew induces the degradation of host chloroplasts.**

A) 3D illustration of the powdery mildew haustorium associated with host chloroplasts at 5dpi. B) TEM image of the haustorium. Note this slice does not include the haustorium neck. C) TEM image, slice includes epidermal chloroplast and mesophyll chloroplast associated with the haustorium. D) Zoom-in TEM image, haustorium adjacent epidermal chloroplast. E) Zoom-in TEM image, haustorium adjacent mesophyll chloroplast. Chl, Chloroplast; EHM, Extrahaustorial Membrane; EMX, Extrahaustorial Matix; HB, Haustorium Body; HL, Haustorium Lobe; LB, Lipid Body; M, Mitochondria; PCW, Plant Cell Wall; PM, Plasma Membrane.

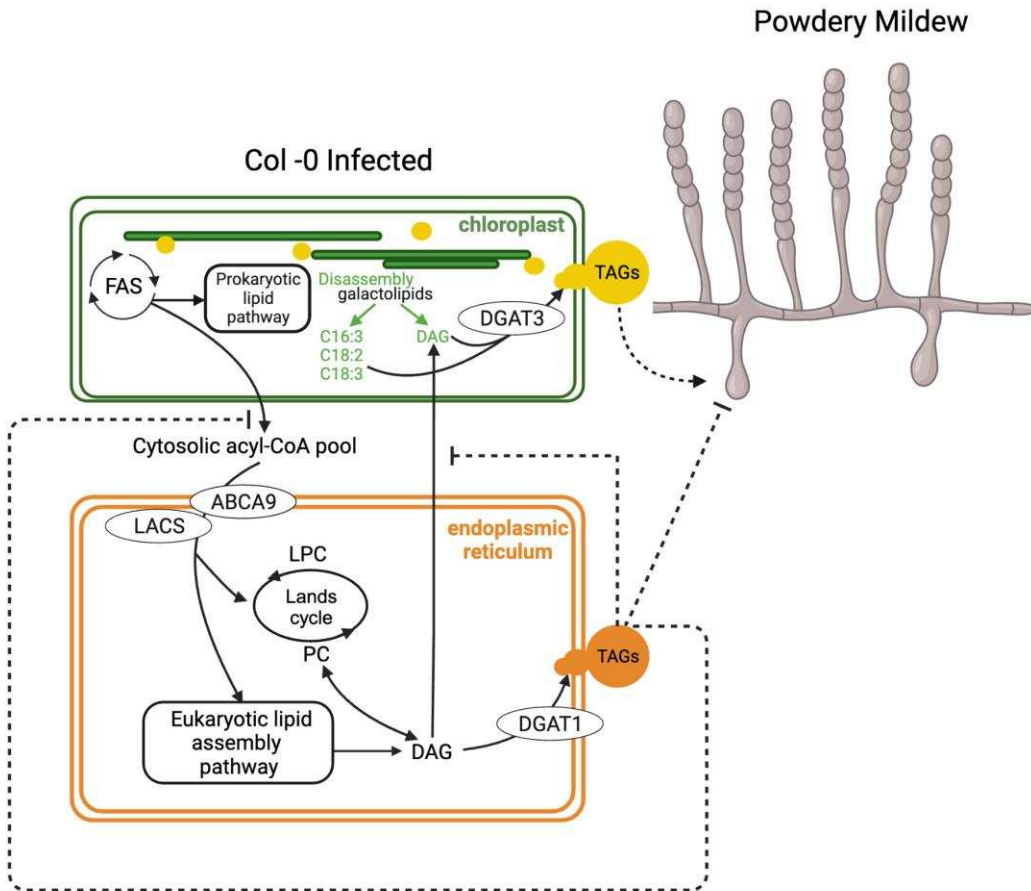


**Figure 7. Simplified model for host lipid metabolism rewiring by powdery mildew during its asexual reproduction.**

Infected *Arabidopsis* leaves have increased abundance of TAGs and chloroplast-associated and cytosolic lipid bodies concurrent with degradation of thylakoid membranes. In addition, confocal imaging suggests the plastid lipid bodies bleb into the cytosol as shown. Thylakoid lipids and derived fatty acids (FA) decrease with infection and are incorporated into accumulated TAGs. Plastidic TAGs are mostly synthesized by the chloroplast-localized AtDGAT3, which prefers C18:3 and C18:2 substrates, and have a unique profile compared to ER TAGs. Plastid DAGs may be derived from thylakoid membrane breakdown and/or import of DAG/DAG precursors from the ER. Knockdown of *DGAT3* and mutation of *DGAT3* reduced powdery mildew spore production, indicating its function benefits the fungus, likely by supplying energy dense lipids for asexual reproduction and/or providing precursors for a fungal reproductive signal. In contrast, TAGs synthesized via DGAT1 in the ER hinder powdery mildew spore production as assessed using knockouts in the ER fatty acid importer *AtABCA9* and *AtDGAT1*. It is likely that multiple ER LACS activate imported FAs as a knockout in *AtLACS1* alone was insufficient to alter powdery mildew spore production. AtPDAT1 and AtDGAT2, known to use a distinct ER DAG pool for TAG synthesis, do not contribute to powdery mildew asexual reproduction and are not included in the model. ER TAG synthesis via DGAT1 may reduce powdery mildew spore production by limiting substrates for plastidic TAG synthesis and/or supplying lipid droplets that contain TAGs and defensive compounds. Abbreviations: ABCA, ATP-binding cassette A; DAG, diacylglycerol; DGAT, diacylglycerol acyltransferase; FAS, fatty acid synthase complex; LACS, long chain acyl-CoA synthetase; LPC, lysoPC; PC, phosphatidylcholine; PDAT, phospholipid:diacylglycerol acyltransferase; TAGs, triacylglycerols. Dashed lines = proposed.

## Parsed Citations

Abood, J. K., and Dorothy M. Lösel. 1989. "Effects of Powdery Mildew Infection on the Lipid Metabolism of Cucumber." In *Biological Role of Plant Lipids*, edited by Péter A. Biacs, Katalin Gruiz, and Tibor Kremmer, 597–601. Boston, MA: Springer US. Google Scholar: [Author Only](#) [Title Only](#) [Author and Title](#)

Arzac, Miren I., Beatriz Fernández-Marín, and José I. García-Plazaola. 2022. "More than Just Lipid Balls: Quantitative Analysis of Plastoglobule Attributes and Their Stress-Related Responses." *Planta* 255 (3): 62.

Atella, Georgia C., Paula R. Bittencourt-Cunha, Rodrigo D. Nunes, Mohammed Shahabuddin, and Mário A. C. Silva-Neto. 2009. "The Major Insect Lipoprotein Is a Lipid Source to Mosquito Stages of Malaria Parasite." *Acta Tropica* 109 (2): 159–62. Google Scholar: [Author Only](#) [Title Only](#) [Author and Title](#)

Aymé, Laure, Simon Arragain, Michel Canonge, Sébastien Baud, Nadia Touati, Ornella Bimai, Franjo Jagic, et al. 2018. "Arabidopsis Thaliana DGAT3 Is a [2Fe-2S] Protein Involved in TAG Biosynthesis." *Scientific Reports* 8 (1): 1–10. Google Scholar: [Author Only](#) [Title Only](#) [Author and Title](#)

Aymé, Laure, Sébastien Baud, Bertrand Dubreucq, Florent Joffre, and Thierry Chardot. 2014. "Function and Localization of the Arabidopsis Thaliana Diacylglycerol Acyltransferase DGAT2 Expressed in Yeast." *PLoS One* 9 (3): e92237. Google Scholar: [Author Only](#) [Title Only](#) [Author and Title](#)

Bates, Philip D. 2022. "Chapter Six - The Plant Lipid Metabolic Network for Assembly of Diverse Triacylglycerol Molecular Species." In *Advances in Botanical Research*, edited by Fabrice Rébeillé and Eric Maréchal, 101:225–52. Academic Press. Google Scholar: [Author Only](#) [Title Only](#) [Author and Title](#)

Bates, Philip D., and John Browse. 2012. "The Significance of Different Diacylglycerol Synthesis Pathways on Plant Oil Composition and Bioengineering." *Frontiers in Plant Science* 3 (July): 147.

Baud, Sébastien, Bertrand Dubreucq, Martine Miquel, Christine Rochat, and Loïc Lepiniec. 2008. "Storage Reserve Accumulation in Arabidopsis: Metabolic and Developmental Control of Seed Filling." *The Arabidopsis Book / American Society of Plant Biologists* 6 (July): e0113. Google Scholar: [Author Only](#) [Title Only](#) [Author and Title](#)

Besagni, Céline, and Felix Kessler. 2013. "A Mechanism Implicating Plastoglobules in Thylakoid Disassembly during Senescence and Nitrogen Starvation." *Planta* 237 (2): 463–70. Google Scholar: [Author Only](#) [Title Only](#) [Author and Title](#)

Both, Maike, Michael Csukai, Michael P. H. Stumpf, and Pietro D. Spanu. 2005. "Gene Expression Profiles of Blumeria Graminis Indicate Dynamic Changes to Primary Metabolism during Development of an Obligate Biotrophic Pathogen." *The Plant Cell* 17 (7): 2107–22. Google Scholar: [Author Only](#) [Title Only](#) [Author and Title](#)

Bouchnak, Imen, Denis Coulon, Vincent Salis, Sabine D'Andréa, and Claire Bréhélin. 2023. "Lipid Droplets Are Versatile Organelles Involved in Plant Development and Plant Response to Environmental Changes." *Frontiers in Plant Science* 14 (June): 1193905. Google Scholar: [Author Only](#) [Title Only](#) [Author and Title](#)

Browse, J., L. Kunst, S. Anderson, S. Hugly, and C. Somerville. 1989. "A Mutant of Arabidopsis Deficient in the Chloroplast 16:1/18:1 Desaturase." *Plant Physiology* 90 (2): 522–29. Google Scholar: [Author Only](#) [Title Only](#) [Author and Title](#)

Browse, J., N. Warwick, C. R. Somerville, and C. R. Slack. 1986. "Fluxes through the Prokaryotic and Eukaryotic Pathways of Lipid Synthesis in the '16:3' Plant Arabidopsis Thaliana." *Biochemical Journal* 235 (1): 25–31. Google Scholar: [Author Only](#) [Title Only](#) [Author and Title](#)

Cavaco, Ana Rita, Ana Rita Matos, and Andreia Figueiredo. 2021. "Speaking the Language of Lipids: The Cross-Talk between Plants and Pathogens in Defence and Disease." *Cellular and Molecular Life Sciences: CMLS* 78 (9): 4399–4415. Google Scholar: [Author Only](#) [Title Only](#) [Author and Title](#)

Chandran, Divya, Noriko Inada, Greg Hather, Christiane K. Kleindt, and Mary C. Wildermuth. 2010. "Laser Microdissection of Arabidopsis Cells at the Powdery Mildew Infection Site Reveals Site-Specific Processes and Regulators." *Proceedings of the National Academy of Sciences of the United States of America* 107 (1): 460–65. Google Scholar: [Author Only](#) [Title Only](#) [Author and Title](#)

Chandran, Divya, Yu Chuan Tai, Gregory Hather, Julia Dewdney, Carine Denoux, Diane G. Burgess, Frederick M. Ausubel, Terence P. Speed, and Mary C. Wildermuth. 2009. "Temporal Global Expression Data Reveal Known and Novel Salicylate-Impacted Processes and Regulators Mediating Powdery Mildew Growth and Reproduction on Arabidopsis." *Plant Physiology* 149 (3): 1435–51. Google Scholar: [Author Only](#) [Title Only](#) [Author and Title](#)

Clark, Joanna I. M., and J. L. Hall. 1998. "Solute Transport into Healthy and Powdery Mildew-Infected Leaves of Pea and Uptake by Powdery Mildew Mycelium." *The New Phytologist* 140 (2): 261–69.

Google Scholar: [Author Only](#) [Title Only](#) [Author and Title](#)

Clay, Nicole K., Adewale M. Adio, Carine Denoux, Georg Jander, and Frederick M. Ausubel. 2009. "Glucosinolate Metabolites Required for an *Arabidopsis* Innate Immune Response." *Science* 323 (5910): 95–101.

Google Scholar: [Author Only](#) [Title Only](#) [Author and Title](#)

Costa, G., M. Gildenhard, M. Eldering, R. L. Lindquist, A. E. Hauser, R. Sauerwein, C. Goosmann, V. Brinkmann, P. Carrillo-Bustamante, and E. A. Levashina. 2018. "Non-Competitive Resource Exploitation within Mosquito Shapes within-Host Malaria Infectivity and Virulence." *Nature Communications* 9 (1): 1–11.

Google Scholar: [Author Only](#) [Title Only](#) [Author and Title](#)

Dahlqvist, Anders, Ulf Ståhl, Marit Lenman, Antoni Banas, Michael Lee, Line Sandager, Hans Ronne, and Sten Stymne. 2000. "Phospholipid:diacylglycerol Acyltransferase: An Enzyme That Catalyzes the Acyl-CoA-Independent Formation of Triacylglycerol in Yeast and Plants." *Proceedings of the National Academy of Sciences* 97 (12): 6487–92.

Google Scholar: [Author Only](#) [Title Only](#) [Author and Title](#)

Devaiah, Shivakumar Pattada, Mary R. Roth, Ethan Baughman, Maoyin Li, Pamela Tamura, Richard Jeannotte, Ruth Welti, and Xuemin Wang. 2006. "Quantitative Profiling of Polar Glycerolipid Species from Organs of Wild-Type *Arabidopsis* and a Phospholipase D $\alpha$ 1 Knockout Mutant." *Phytochemistry* 67 (17): 1907–24.

Google Scholar: [Author Only](#) [Title Only](#) [Author and Title](#)

Espinosa-Corral, Roberto, Serena Schwenkert, and Peter K. Lundquist. 2021. "Molecular Changes of *Arabidopsis Thaliana* Plastoglobules Facilitate Thylakoid Membrane Remodeling under High Light Stress." *The Plant Journal: For Cell and Molecular Biology* 106 (6): 1571–87.

Google Scholar: [Author Only](#) [Title Only](#) [Author and Title](#)

Fan, Jian, Chengshi Yan, and Changcheng Xu. 2013. "Phospholipid:diacylglycerol Acyltransferase-Mediated Triacylglycerol Biosynthesis Is Crucial for Protection against Fatty Acid-Induced Cell Death in Growing Tissues of *Arabidopsis*." *The Plant Journal: For Cell and Molecular Biology* 76 (6): 930–42.

Google Scholar: [Author Only](#) [Title Only](#) [Author and Title](#)

Fernández-Santos, Rubén, Yovanny Izquierdo, Ana López, Luis Muñiz, Marta Martínez, Tomás Cascón, Mats Hamberg, and Carmen Castresana. 2020. "Protein Profiles of Lipid Droplets during the Hypersensitive Defense Response of *Arabidopsis* against *Pseudomonas* Infection." *Plant & Cell Physiology* 61 (6): 1144–57.

Google Scholar: [Author Only](#) [Title Only](#) [Author and Title](#)

Fotopoulos, Vasileios, Martin J. Gilbert, Jon K. Pittman, Alison C. Marvier, Aram J. Buchanan, Norbert Sauer, J. L. Hall, and Lorraine E. Williams. 2003. "The Monosaccharide Transporter Gene, AtSTP4, and the Cell-Wall Invertase, Atbetafruct1, Are Induced in *Arabidopsis* during Infection with the Fungal Biotroph *Erysiphe Cichoracearum*." *Plant Physiology* 132 (2): 821–29.

Google Scholar: [Author Only](#) [Title Only](#) [Author and Title](#)

Frye, C. A., and R. W. Innes. 1998. "An *Arabidopsis* Mutant with Enhanced Resistance to Powdery Mildew." *The Plant Cell* 10 (6): 947–56.

Google Scholar: [Author Only](#) [Title Only](#) [Author and Title](#)

Frye, Catherine A, Dingzhong Tang, and Roger W. Innes. 2001. "Negative Regulation of Defense Responses in Plants by a Conserved MAPKK Kinase." *Proceedings of the National Academy of Sciences* 98 (1): 373–78.

Google Scholar: [Author Only](#) [Title Only](#) [Author and Title](#)

Gao, Huiling, Yu Gao, Fei Zhang, Baoling Liu, Chunli Ji, Jinai Xue, Lixia Yuan, and Runzhi Li. 2021. "Functional Characterization of a Novel Acyl-CoA:diacylglycerol Acyltransferase 3-3 (CsDGAT3-3) Gene from *Camelina Sativa*." *Plant Science: An International Journal of Experimental Plant Biology* 303 (February): 110752.

Google Scholar: [Author Only](#) [Title Only](#) [Author and Title](#)

Gaude, Nicole, Claire Bréhélin, Gilbert Tischendorf, Felix Kessler, and Peter Dörmann. 2007. "Nitrogen Deficiency in *Arabidopsis* Affects Galactolipid Composition and Gene Expression and Results in Accumulation of Fatty Acid Phytol Esters." *The Plant Journal: For Cell and Molecular Biology* 49 (4): 729–39.

Google Scholar: [Author Only](#) [Title Only](#) [Author and Title](#)

Ghosh, S., K. A. Hudak, E. B. Dumbroff, and J. E. Thompson. 1994. "Release of Photosynthetic Protein Catabolites by Blebbing from Thylakoids." *Plant Physiology* 106 (4): 1547–53.

Google Scholar: [Author Only](#) [Title Only](#) [Author and Title](#)

Glawe, Dean A. 2008. "The Powdery Mildews: A Review of the World's Most Familiar (yet Poorly Known) Plant Pathogens." *Annual Review of Phytopathology* 46: 27–51.

Google Scholar: [Author Only](#) [Title Only](#) [Author and Title](#)

Guzha, Athanas, Payton Whitehead, Till Ischebeck, and Kent D. Chapman. 2023. "Lipid Droplets: Packing Hydrophobic Molecules

**Within the Aqueous Cytoplasm." Annual Review of Plant Biology 74 (1): 195–223.**

Google Scholar: [Author Only](#) [Title Only](#) [Author and Title](#)

**Han, Longyan, Yuhui Zhai, Yumeng Wang, Xiangrui Shi, Yanfeng Xu, Shuguang Gao, Man Zhang, Jianrang Luo, and Qingyu Zhang. 2022. "Diacylglycerol Acyltransferase 3(DGAT3) Is Responsible for the Biosynthesis of Unsaturated Fatty Acids in Vegetative Organs of *Paeonia Rockii*." International Journal of Molecular Sciences 23 (22). <https://doi.org/10.3390/ijms232214390>.**

Google Scholar: [Author Only](#) [Title Only](#) [Author and Title](#)

**Hernández, M. Luisa, and Francisco Javier Cejudo. 2021. "Chloroplast Lipids Metabolism and Function. A Redox Perspective." Frontiers in Plant Science 12 (August): 712022.**

Google Scholar: [Author Only](#) [Title Only](#) [Author and Title](#)

**Hernández, M. Luisa, Lynne Whitehead, Zhesi He, Valeria Gazda, Alison Gilday, Ekaterina Kozhevnikova, Fabián E. Vaistij, Tony R. Larson, and Ian A. Graham. 2012. "A Cytosolic Acyltransferase Contributes to Triacylglycerol Synthesis in Sucrose-Rescued *Arabidopsis* Seed Oil Catabolism Mutants." Plant Physiology 160 (1): 215–25.**

Google Scholar: [Author Only](#) [Title Only](#) [Author and Title](#)

**Hölzl, Georg, and Peter Dörmann. 2019. "Chloroplast Lipids and Their Biosynthesis." Annual Review of Plant Biology 70 (April): 51–81.**

Google Scholar: [Author Only](#) [Title Only](#) [Author and Title](#)

**Hunziker, Pascal, Hassan Ghareeb, Lena Wagenknecht, Christoph Crocoll, Barbara Ann Halkier, Volker Lipka, and Alexander Schulz. 2020. "De Novo Indol-3-Ylmethyl Glucosinolate Biosynthesis, and Not Long-Distance Transport, Contributes to Defence of *Arabidopsis* against Powdery Mildew." Plant, Cell & Environment 43 (6): 1571–83.**

Google Scholar: [Author Only](#) [Title Only](#) [Author and Title](#)

**Jessen, Dirk, Charlotte Roth, Marcel Wiermer, and Martin Fulda. 2015. "Two Activities of Long-Chain Acyl-Coenzyme A Synthetase Are Involved in Lipid Trafficking between the Endoplasmic Reticulum and the Plastid in *Arabidopsis*." Plant Physiology 167 (2): 351–66.**

Google Scholar: [Author Only](#) [Title Only](#) [Author and Title](#)

**Jiang, Yina, Wanxiao Wang, Qiujin Xie, Na Liu, Lixia Liu, Dapeng Wang, Xiaowei Zhang, et al. 2017. "Plants Transfer Lipids to Sustain Colonization by Mutualistic Mycorrhizal and Parasitic Fungi." Science 356 (6343): 1172–75.**

Google Scholar: [Author Only](#) [Title Only](#) [Author and Title](#)

**Kachroo, Aardra, and Pradeep Kachroo. 2009. "Fatty Acid-Derived Signals in Plant Defense." Annual Review of Phytopathology 47 (1): 153–76.**

Google Scholar: [Author Only](#) [Title Only](#) [Author and Title](#)

**Kameoka, Hiromu, and Caroline Gutjahr. 2022. "Functions of Lipids in Development and Reproduction of Arbuscular Mycorrhizal Fungi." Plant & Cell Physiology 63 (10): 1356–65.**

Google Scholar: [Author Only](#) [Title Only](#) [Author and Title](#)

**Kameoka, Hiromu, Taro Maeda, Nao Okuma, and Masayoshi Kawaguchi. 2019. "Structure-Specific Regulation of Nutrient Transport and Metabolism in Arbuscular Mycorrhizal Fungi." Plant & Cell Physiology 60 (10): 2272–81.**

Google Scholar: [Author Only](#) [Title Only](#) [Author and Title](#)

**Katavic, V., D. W. Reed, D. C. Taylor, E. M. Giblin, D. L. Barton, J. Zou, S. L. Mackenzie, P. S. Covello, and L. Kunst. 1995. "Alteration of Seed Fatty Acid Composition by an Ethyl Methanesulfonate-Induced Mutation in *Arabidopsis Thaliana* Affecting Diacylglycerol Acyltransferase Activity." Plant Physiology 108 (1): 399–409.**

Google Scholar: [Author Only](#) [Title Only](#) [Author and Title](#)

**Kaup, Marianne T., Carol D. Froese, and John E. Thompson. 2002. "A Role for Diacylglycerol Acyltransferase during Leaf Senescence." Plant Physiology 129 (4): 1616–26.**

Google Scholar: [Author Only](#) [Title Only](#) [Author and Title](#)

**Kim, Sangwoo, Yasuyo Yamaoka, Hirofumi Ono, Hanul Kim, Donghwan Shim, Masayoshi Maeshima, Enrico Martinoia, Edgar B. Cahoon, Ikuo Nishida, and Youngsook Lee. 2013. "A ABCA9 Transporter Supplies Fatty Acids for Lipid Synthesis to the Endoplasmic Reticulum." Proceedings of the National Academy of Sciences of the United States of America 110 (2): 773–78.**

Google Scholar: [Author Only](#) [Title Only](#) [Author and Title](#)

**Klepikova, Anna V., Artem S. Kasianov, Evgeny S. Gerasimov, Maria D. Logacheva, and Aleksey A. Penin. 2016. "A High Resolution Map of the *Arabidopsis Thaliana* Developmental Transcriptome Based on RNA-Seq Profiling." The Plant Journal: For Cell and Molecular Biology 88 (6): 1058–70.**

Google Scholar: [Author Only](#) [Title Only](#) [Author and Title](#)

**Koh, Serry, Aurélie André, Herb Edwards, David Ehrhardt, and Shauna Somerville. 2005. "Arabidopsis Thaliana Subcellular Responses to Compatible Erysiphe Cichoracearum Infections." The Plant Journal: For Cell and Molecular Biology 44 (3): 516–29.**

Google Scholar: [Author Only](#) [Title Only](#) [Author and Title](#)

**Kumar, Aruna, Aarti Sharma, and Kailash C. Upadhyaya. 2016. "Vegetable Oil: Nutritional and Industrial Perspective." Current Genomics 17 (3): 230–40.**

Google Scholar: [Author Only](#) [Title Only](#) [Author and Title](#)

**Liang, Peng, Songyu Liu, Feng Xu, Shuqin Jiang, Jun Yan, Qiguang He, Wenbo Liu, et al. 2018. "Powdery Mildews Are Characterized by Contracted Carbohydrate Metabolism and Diverse Effectors to Adapt to Obligate Biotrophic Lifestyle." Frontiers in Microbiology 9 (December): 3160.**

Google Scholar: [Author Only](#) [Title Only](#) [Author and Title](#)

**Lippold, Felix, Katharina vom Dorp, Marion Abraham, Georg Hözl, Vera Wewer, Jenny Lindberg Yilmaz, Ida Lager, et al. 2012. "Fatty Acid Phytol Ester Synthesis in Chloroplasts of Arabidopsis." The Plant Cell 24 (5): 2001–14.**

Google Scholar: [Author Only](#) [Title Only](#) [Author and Title](#)

**Liu, Simu, Lisa M. Bartrikas, Sigrid M. Volk, Frederick M. Ausubel, and Dingzhong Tang. 2016. "Mutation of the Glucosinolate Biosynthesis Enzyme Cytochrome P450 83A1 Monooxygenase Increases Camalexin Accumulation and Powdery Mildew Resistance." Frontiers in Plant Science 7 (March): 227.**

**Luginbuehl, Leonie H., Guillaume N. Menard, Smita Kurup, Harrie Van Erp, Guru V. Radhakrishnan, Andrew Breakspear, Giles E. D. Oldroyd, and Peter J. Eastmond. 2017. "Fatty Acids in Arbuscular Mycorrhizal Fungi Are Synthesized by the Host Plant." Science 356 (6343): 1175–78.**

Google Scholar: [Author Only](#) [Title Only](#) [Author and Title](#)

**Lu, Junhao, Yang Xu, Juli Wang, Stacy D. Singer, and Guanqun Chen. 2020. "The Role of Triacylglycerol in Plant Stress Response." Plants 9 (4). <https://doi.org/10.3390/plants9040472>.**

Google Scholar: [Author Only](#) [Title Only](#) [Author and Title](#)

**Lundquist, Peter K., Anton Poliakov, Nazmul H. Bhuiyan, Boris Zybailov, Qi Sun, and Klaas J. van Wijk. 2012. "The Functional Network of the Arabidopsis Plastoglobule Proteome Based on Quantitative Proteomics and Genome-Wide Coexpression Analysis." Plant Physiology 158 (3): 1172–92.**

Google Scholar: [Author Only](#) [Title Only](#) [Author and Title](#)

**Lü, Shiyu, Tao Song, Dylan K. Kosma, Eugene P. Parsons, Owen Rowland, and Matthew A. Jenks. 2009. "Arabidopsis CER8 Encodes LONG-CHAIN ACYL-COA SYNTHETASE 1 (LACS1) That Has Overlapping Functions with LACS2 in Plant Wax and Cutin Synthesis." The Plant Journal: For Cell and Molecular Biology 59 (4): 553–64.**

Google Scholar: [Author Only](#) [Title Only](#) [Author and Title](#)

**MacLean, Allyson M., Armando Bravo, and Maria J. Harrison. 2017. "Plant Signaling and Metabolic Pathways Enabling Arbuscular Mycorrhizal Symbiosis." The Plant Cell 29 (10): 2319–35.**

Google Scholar: [Author Only](#) [Title Only](#) [Author and Title](#)

**Mats X. Andersson, J. Magnus Kjellberg, and Anna Stina Sandelius. 2001. "Chloroplast Biogenesis. Regulation of Lipid Transport to the Thylakoid in Chloroplasts Isolated from Expanding and Fully Expanded Leaves of Pea." Plant Physiology 127 (1): 184–93.**

Google Scholar: [Author Only](#) [Title Only](#) [Author and Title](#)

**McRae, Amanda G., Jyoti Taneja, Kathleen Yee, Xinyi Shi, Sajeet Haridas, Kurt LaButti, Vasanth Singan, Igor V. Grigoriev, and Mary C. Wildermuth. 2023. "Spray-Induced Gene Silencing to Identify Powdery Mildew Gene Targets and Processes for Powdery Mildew Control." Molecular Plant Pathology 24 (9): 1168–83.**

Google Scholar: [Author Only](#) [Title Only](#) [Author and Title](#)

**Micali, Cristina, Katharina Göllner, Matt Humphry, Chiara Consonni, and Ralph Panstruga. 2008. "The Powdery Mildew Disease of Arabidopsis: A Paradigm for the Interaction between Plants and Biotrophic Fungi." The Arabidopsis Book / American Society of Plant Biologists 6 (October): e0115.**

Google Scholar: [Author Only](#) [Title Only](#) [Author and Title](#)

**Michel, Elena J. S., Lalit Ponnala, and Klaas J. van Wijk. 2021. "Tissue-Type Specific Accumulation of the Plastoglobular Proteome, Transcriptional Networks, and Plastoglobular Functions." Journal of Experimental Botany 72 (13): 4663–79.**

Google Scholar: [Author Only](#) [Title Only](#) [Author and Title](#)

**Moellering, Eric R., Bagyalakshmi Muthan, and Christoph Benning. 2010. "Freezing Tolerance in Plants Requires Lipid Remodeling at the Outer Chloroplast Membrane." Science 330 (6001): 226–28.**

Google Scholar: [Author Only](#) [Title Only](#) [Author and Title](#)

**Murphy, Robert C. 2014. Tandem Mass Spectrometry of Lipids: Molecular Analysis of Complex Lipids. Royal Society of Chemistry.**

Google Scholar: [Author Only](#) [Title Only](#) [Author and Title](#)

**Okazaki, Yozo, and Kazuki Saito. 2014. "Roles of Lipids as Signaling Molecules and Mitigators during Stress Response in Plants." The Plant Journal: For Cell and Molecular Biology 79 (4): 584–96.**

Google Scholar: [Author Only](#) [Title Only](#) [Author and Title](#)

**Pfleger, Brian F., Michael Gossing, and Jens Nielsen. 2015. "Metabolic Engineering Strategies for Microbial Synthesis of**

## Oleochemicals." *Metabolic Engineering* 29 (May): 1–11.

Google Scholar: [Author Only](#) [Title Only](#) [Author and Title](#)

Przybyla-Toscano, Jonathan, Mélanie Roland, Frédéric Gaynard, Jérémy Couturier, and Nicolas Rouhier. 2018. "Roles and Maturation of Iron-Sulfur Proteins in Plastids." *Journal of Biological Inorganic Chemistry: JBIC: A Publication of the Society of Biological Inorganic Chemistry* 23 (4): 545–66.

Google Scholar: [Author Only](#) [Title Only](#) [Author and Title](#)

Regmi, Anushobha, Jay Shockey, Hari Kiran Kotapati, and Philip D. Bates. 2020. "Oil-Producing Metabolons Containing DGAT1 Use Separate Substrate Pools from Those Containing DGAT2 or PDAT." *Plant Physiology* 184 (2): 720–37.

Google Scholar: [Author Only](#) [Title Only](#) [Author and Title](#)

Reuber, T. L., J. M. Plotnikova, J. Dewdney, E. E. Rogers, W. Wood, and F. M. Ausubel. 1998. "Correlation of Defense Gene Induction Defects with Powdery Mildew Susceptibility in *Arabidopsis* Enhanced Disease Susceptibility Mutants." *The Plant Journal: For Cell and Molecular Biology* 16 (4): 473–85.

Google Scholar: [Author Only](#) [Title Only](#) [Author and Title](#)

Saha, Saikat, Balaji Enugutti, Sona Rajakumari, and Ram Rajasekharan. 2006. "Cytosolic Triacylglycerol Biosynthetic Pathway in Oilseeds. Molecular Cloning and Expression of Peanut Cytosolic Diacylglycerol Acyltransferase." *Plant Physiology* 141 (4): 1533–43.

Google Scholar: [Author Only](#) [Title Only](#) [Author and Title](#)

Shimada, Takashi L., Makoto Hayashi, and Ikuko Hara-Nishimura. 2017. "Membrane Dynamics and Multiple Functions of Oil Bodies in Seeds and Leaves." *Plant Physiology* 176 (1): 199–207.

Google Scholar: [Author Only](#) [Title Only](#) [Author and Title](#)

Shimada, Takashi L., Yoshitaka Takano, Tomoo Shimada, Masayuki Fujiwara, Yoichiro Fukao, Masashi Mori, Yozo Okazaki, et al. 2014. "Leaf Oil Body Functions as a Subcellular Factory for the Production of a Phytoalexin in *Arabidopsis*." *Plant Physiology* 164 (1): 105–18.

Google Scholar: [Author Only](#) [Title Only](#) [Author and Title](#)

Shiva, Sunitha, Thilani Samarakoon, Kaleb A. Lowe, Charles Roach, Hieu Sy Vu, Madeline Colter, Hollie Porras, et al. 2020. "Leaf Lipid Alterations in Response to Heat Stress of *Arabidopsis Thaliana*." *Plants* 9 (7). <https://doi.org/10.3390/plants9070845>.

Google Scholar: [Author Only](#) [Title Only](#) [Author and Title](#)

Shiva, Sunitha, Hieu Sy Vu, Mary R. Roth, Zhenguo Zhou, Shantan Reddy Marepally, Daya Sagar Nune, Gerald H. Lushington, Mahesh Visvanathan, and Ruth Welti. 2013. "Lipidomic Analysis of Plant Membrane Lipids by Direct Infusion Tandem Mass Spectrometry." *Methods in Molecular Biology* 1009: 79–91.

Google Scholar: [Author Only](#) [Title Only](#) [Author and Title](#)

Smith, Matthew D., Donny D. Licatalosi, and John E. Thompson. 2000. "Co-Association of Cytochrome F Catabolites and Plastid-Lipid-Associated Protein with Chloroplast Lipid Particles1." *Plant Physiology* 124 (1): 211–22.

Google Scholar: [Author Only](#) [Title Only](#) [Author and Title](#)

Spanu, Pietro D. 2012. "The Genomics of Obligate (and Nonobligate) Biotrophs." *Annual Review of Phytopathology* 50 (May): 91–109.

Google Scholar: [Author Only](#) [Title Only](#) [Author and Title](#)

Springer, Armin, Chulhee Kang, Sachin Rustgi, Diter von Wettstein, Christiane Reinbothe, Stephan Pollmann, and Steffen Reinbothe. 2016. "Programmed Chloroplast Destruction during Leaf Senescence Involves 13-Lipoxygenase (13-LOX)." *Proceedings of the National Academy of Sciences* 113 (12): 3383–88.

Google Scholar: [Author Only](#) [Title Only](#) [Author and Title](#)

Sutton, P. N., M. J. Henry, and J. L. Hall. 1999. "Glucose, and Not Sucrose, Is Transported from Wheat to Wheat Powdery Mildew." *Planta* 208 (3): 426–30.

Google Scholar: [Author Only](#) [Title Only](#) [Author and Title](#)

Swarbrick, Philip J., Paul Schulze-Lefert, and Julie D. Scholes. 2006. "Metabolic Consequences of Susceptibility and Resistance (race-Specific and Broad-Spectrum) in Barley Leaves Challenged with Powdery Mildew." *Plant, Cell & Environment* 29 (6): 1061–76.

Google Scholar: [Author Only](#) [Title Only](#) [Author and Title](#)

Tang, Dingzhong, Michael T. Simonich, and Roger W. Innes. 2007. "Mutations in LACS2, a Long-Chain Acyl-Coenzyme A Synthetase, Enhance Susceptibility to Avirulent *Pseudomonas Syringae* but Confer Resistance to *Botrytis Cinerea* in *Arabidopsis*." *Plant Physiology* 144 (2): 1093–1103.

Google Scholar: [Author Only](#) [Title Only](#) [Author and Title](#)

Tournayre, Jeremy, Matthieu Reichstadt, Laurent Parry, Pierre Fafournoux, and Celine Jousse. 2019. "'Do My qPCR Calculation', a Web Tool." *Bioinformation* 15 (5): 369–72.

Google Scholar: [Author Only](#) [Title Only](#) [Author and Title](#)

**Tsitsigiannis, Dimitrios I., Terri M. Kowieski, Robert Zarnowski, and Nancy P. Keller.** 2004. "Endogenous Lipogenic Regulators of Spore Balance in *Aspergillus nidulans*." *Eukaryotic Cell* 3 (6): 1398–1411.

Google Scholar: [Author Only](#) [Title Only](#) [Author and Title](#)

**Vallochi, Adriana Lima, Livia Teixeira, Karina da Silva Oliveira, Clarissa Menezes Maya-Monteiro, and Patricia T. Bozza.** 2018. "Lipid Droplet, a Key Player in Host-Parasite Interactions." *Frontiers in Immunology* 9 (May): 1022.

Google Scholar: [Author Only](#) [Title Only](#) [Author and Title](#)

**Vanhercke, Thomas, John M. Dyer, Robert T. Mullen, Aruna Kilaru, Md Mahbubur Rahman, James R. Petrie, Allan G. Green, Olga Yurchenko, and Surinder P. Singh.** 2019. "Metabolic Engineering for Enhanced Oil in Biomass." *Progress in Lipid Research* 74 (April): 103–29.

Google Scholar: [Author Only](#) [Title Only](#) [Author and Title](#)

**Vanhercke, Thomas, Anna El Tahchy, Pushkar Shrestha, Xue-Rong Zhou, Surinder P. Singh, and James R. Petrie.** 2013. "Synergistic Effect of WRI1 and DGAT1 Coexpression on Triacylglycerol Biosynthesis in Plants." *FEBS Letters* 587 (4): 364–69.

Google Scholar: [Author Only](#) [Title Only](#) [Author and Title](#)

**Vidi, Pierre-Alexandre, Marion Kanwischer, Sacha Baginsky, Jotham R. Austin, Gabor Csucs, Peter Dörmann, Felix Kessler, and Claire Bréhélin.** 2006. "Tocopherol Cyclase (VTE1) Localization and Vitamin E Accumulation in Chloroplast Plastoglobule Lipoprotein Particles." *The Journal of Biological Chemistry* 281 (16): 11225–34.

Google Scholar: [Author Only](#) [Title Only](#) [Author and Title](#)

**Wang, Liping, Wenyun Shen, Michael Kazachkov, Guanqun Chen, Qilin Chen, Anders S. Carlsson, Sten Stymne, Randall J. Weselake, and Jitao Zou.** 2012. "Metabolic Interactions between the Lands Cycle and the Kennedy Pathway of Glycerolipid Synthesis in *Arabidopsis* Developing Seeds." *The Plant Cell* 24 (11): 4652–69.

Google Scholar: [Author Only](#) [Title Only](#) [Author and Title](#)

**Wang, Wenming, Yingqiang Wen, Robert Berkey, and Shunyuan Xiao.** 2009. "Specific Targeting of the *Arabidopsis* Resistance Protein RPW8.2 to the Interfacial Membrane Encasing the Fungal Haustorium Renders Broad-Spectrum Resistance to Powdery Mildew." *The Plant Cell* 21 (9): 2898–2913.

Google Scholar: [Author Only](#) [Title Only](#) [Author and Title](#)

**Welti, Ruth, Weiqi Li, Maoyin Li, Yongming Sang, Homigol Biesiada, Han-E Zhou, C. B. Rajashekhar, Todd D. Williams, and Xuemin Wang.** 2002. "Profiling Membrane Lipids in Plant Stress Responses. Role of Phospholipase D Alpha in Freezing-Induced Lipid Changes in *Arabidopsis*." *The Journal of Biological Chemistry* 277 (35): 31994–2.

Google Scholar: [Author Only](#) [Title Only](#) [Author and Title](#)

**Weng, Hua, Isabel Molina, Jay Shockey, and John Browse.** 2010. "Organ Fusion and Defective Cuticle Function in a lacs1 lacs2 Double Mutant of *Arabidopsis*." *Planta* 231 (5): 1089–1100.

Google Scholar: [Author Only](#) [Title Only](#) [Author and Title](#)

**Weßling, Ralf, and Ralph Panstruga.** 2012. "Rapid Quantification of Plant-Powdery Mildew Interactions by qPCR and Conidiospore Counts." *Plant Methods* 8 (1): 35.

**Wildermuth, Mary C.** 2010. "Modulation of Host Nuclear Ploidy: A Common Plant Biotroph Mechanism." *Current Opinion in Plant Biology* 13 (4): 449–58.

Google Scholar: [Author Only](#) [Title Only](#) [Author and Title](#)

**Wildermuth, Mary C., Michael A. Steinwand, Amanda G. McRae, Johan Jaenisch, and Divya Chandran.** 2017. "Adapted Biotroph Manipulation of Plant Cell Ploidy." *Annual Review of Phytopathology* 55 (August): 537–64.

Google Scholar: [Author Only](#) [Title Only](#) [Author and Title](#)

**Winter, Debbie, Ben Vinegar, Hardeep Nahal, Ron Ammar, Greg V. Wilson, and Nicholas J. Provart.** 2007. "An 'Electronic Fluorescent Pictograph' Browser for Exploring and Analyzing Large-Scale Biological Data Sets." *PLoS One* 2 (8): e718.

**Xu, Changcheng, Julian Fan, and John Shanklin.** 2020. "Metabolic and Functional Connections between Cytoplasmic and Chloroplast Triacylglycerol Storage." *Progress in Lipid Research* 80 (November): 101069.

Google Scholar: [Author Only](#) [Title Only](#) [Author and Title](#)

**Xu, Changcheng, and John Shanklin.** 2016. "Triacylglycerol Metabolism, Function, and Accumulation in Plant Vegetative Tissues." *Annual Review of Plant Biology* 67 (April): 179–206.

Google Scholar: [Author Only](#) [Title Only](#) [Author and Title](#)

**Xue, Jinai, Huiling Gao, Yinghong Xue, Ruixiang Shi, Mengmeng Liu, Lijun Han, Yu Gao, et al.** 2022. "Functional Characterization of Soybean Diacylglycerol Acyltransferase 3 in Yeast and Soybean." *Frontiers in Plant Science* 13 (May): 854103.

Google Scholar: [Author Only](#) [Title Only](#) [Author and Title](#)

**Xu, Xiao-Yu, Hong-Kun Yang, Surinder P. Singh, Peter J. Sharp, and Qing Liu.** 2018. "Genetic Manipulation of Non-Classic Oilseed Plants for Enhancement of Their Potential as a Biofactory for Triacylglycerol Production." *Proceedings of the Estonian Academy of Sciences: Engineering* 4 (4): 523–33.

Google Scholar: [Author Only](#) [Title Only](#) [Author and Title](#)

**Yan, Bowei, Xiaoxuan Xu, Yingnan Gu, Ying Zhao, Xunchao Zhao, Lin He, Changjiang Zhao, Zutong Li, and Jingyu Xu. 2018. "Genome-Wide Characterization and Expression Profiling of Diacylglycerol Acyltransferase Genes from Maize." *Genome / National Research Council Canada = Genome / Conseil National de Recherches Canada* 61 (10): 735–43.**

Google Scholar: [Author Only](#) [Title Only](#) [Author and Title](#)

**Yao, Hong-Yan, Yao-Qi Lu, Xiao-Li Yang, Xiao-Qing Wang, Zhipu Luo, De-Li Lin, Jia-Wei Wu, and Hong-Wei Xue. 2023. "Arabidopsis Sec14 Proteins (SFH5 and SFH7) Mediate Interorganelle Transport of Phosphatidic Acid and Regulate Chloroplast Development." *Proceedings of the National Academy of Sciences of the United States of America* 120 (6): e2221637120.**

Google Scholar: [Author Only](#) [Title Only](#) [Author and Title](#)

**Yin, Xiangzhen, Xupeng Guo, Lizong Hu, Shuangshuang Li, Yuhong Chen, Jingqiao Wang, Richard R-C Wang, Chengming Fan, and Zanmin Hu. 2022. "Genome-Wide Characterization of DGATs and Their Expression Diversity Analysis in Response to Abiotic Stresses in Brassica Napus." *Plants* 11 (9). <https://doi.org/10.3390/plants11091156>.**

Google Scholar: [Author Only](#) [Title Only](#) [Author and Title](#)

**Ytterberg, A. Jimmy, Jean-Benoit Peltier, and Klaas J. van Wijk. 2006. "Protein Profiling of Plastoglobules in Chloroplasts and Chromoplasts. A Surprising Site for Differential Accumulation of Metabolic Enzymes." *Plant Physiology* 140 (3): 984–97.**

Google Scholar: [Author Only](#) [Title Only](#) [Author and Title](#)

**Zhang, Meng, Julian Fan, David C. Taylor, and John B. Ohlrogge. 2009. "DGAT1 and PDAT1 Acyltransferases Have Overlapping Functions in Arabidopsis Triacylglycerol Biosynthesis and Are Essential for Normal Pollen and Seed Development." *The Plant Cell* 21 (12): 3885–3901.**

Google Scholar: [Author Only](#) [Title Only](#) [Author and Title](#)

**Zhao, Lifang, Vesna Katavic, Fengling Li, George W. Haughn, and Ljerka Kunst. 2010. "Insertional Mutant Analysis Reveals That Long-Chain Acyl-CoA Synthetase 1 (LACS1), but Not LACS8, Functionally Overlaps with LACS9 in Arabidopsis Seed Oil Biosynthesis." *The Plant Journal: For Cell and Molecular Biology* 64 (6): 1048–58.**

Google Scholar: [Author Only](#) [Title Only](#) [Author and Title](#)

**Zhou, Xue-Rong, Sajina Bhandari, Brandon S. Johnson, Hari Kiran Kotapati, Doug K. Allen, Thomas Vanhercke, and Philip D. Bates. 2019. "Reorganization of Acyl Flux through the Lipid Metabolic Network in Oil-Accumulating Tobacco Leaves1 [OPEN]." *Plant Physiology* 182 (2): 739–55.**

Google Scholar: [Author Only](#) [Title Only](#) [Author and Title](#)

**Zhou, Xue-Rong, Pushkar Shrestha, Fang Yin, James R. Petrie, and Surinder P. Singh. 2013. "AtDGAT2 Is a Functional Acyl-CoA:Diacylglycerol Acyltransferase and Displays Different Acyl-CoA Substrate Preferences than AtDGAT1." *FEBS Letters* 587 (15): 2371–76.**

Google Scholar: [Author Only](#) [Title Only](#) [Author and Title](#)

**Zou, J., Y. Wei, C. Jako, A. Kumar, G. Selvaraj, and D. C. Taylor. 1999. "The Arabidopsis Thaliana TAG1 Mutant Has a Mutation in a Diacylglycerol Acyltransferase Gene." *The Plant Journal: For Cell and Molecular Biology* 19 (6): 645–53.**

Google Scholar: [Author Only](#) [Title Only](#) [Author and Title](#)

**Shiva, S., Vu, H. S., Roth, M. R., Zhou, Z., Marepally, S. R., Nune, D. S., Lushington, G. H., Visvanathan, M., & Welti, R. 2013. "Lipidomic analysis of plant membrane lipids by direct infusion tandem mass spectrometry." *Methods in molecular biology* (Clifton, N.J.), 1009, 79–91. [https://doi.org/10.1007/978-1-62703-401-2\\_9](https://doi.org/10.1007/978-1-62703-401-2_9)**

Google Scholar: [Author Only](#) [Title Only](#) [Author and Title](#)